

**Signature of the Multiple Timescales of Memory in Adaptive Control
of Human Saccades**

by

Vincent Ethier

A thesis submitted to The Johns Hopkins University in conformity with the requirements
for the degree of Master of Science in Engineering.

Baltimore, Maryland

May, 2008

© Vincent Ethier 2008

All rights reserved

Abstract

In the past 30 years, saccade experiment has been a motor task favoured by many scientists interested in adaptation and learning. Saccades are stereotypical and less subject to cognitive influences than are motor tasks like reaching. They are also too fast to let sensory feedback affect their control; this consequently makes them simpler to analyze. In addition, their neural correlates have been extensively researched and the principal neural pathways are relatively well-understood.

Saccade adaptation is first utilized here to demonstrate the multiple timescales of oculomotor memory. Thanks to the use of error-clamp trials for saccades, we were able to monitor the state of the learner while minimally interfering with it. The analysis of the spontaneous recovery phenomenon, previously observed in arm-reaching experiments, allowed us to measure the timescales of two memory systems, each learning and forgetting at its own characteristic rate. We show that these rates live in time spaces of different orders of magnitude and hence are qualified as belonging to a 'fast' and a 'slow' system.

The kinematics of saccades made to repetitive targets change in a stereotypical manner while the amplitude remains constant. This 'fatigue' is characterized by slower and

ABSTRACT

longer lasting saccades and occurs with and without target-jump adaptation. We propose an optimal control model of the oculomotor plant that accounts for this reoptimization of the saccade metrics. The concept of 'internal value' of a goal arises naturally from the adjustments of the model that were made in this framework.

Finally, the saccade kinematics of in-axis adaptation are characterized and compared to control profiles using a novel paradigm that mimicks the pattern of saccade adaptation. We suggest that gain-down adaptation relies predominantly on adjustments made by a forward model fed by internal feedback and show that this mechanism of adaptation predicts the drop in speed and increase in duration observed in the data. On the other hand, during gain-up adaptation, saccade profiles were found to be indistinguishable from their controls. We argue that this points to a possible second mechanism of adaptation involving mainly a remapping of the target.

Primary Reader and Advisor: Dr. Reza Shadmehr

Secondary Readers: Dr. David Zee and Dr. Mark Shelhamer

Acknowledgements

I thank Dr. Reza Shadmehr, Dr. David Zee, and the members of the Shadmehr lab, who all played a decisive part in two years of research which culminated in the reflections and scientific findings presented in this essay. I would also like to thank my family: Lyse Ethier, Jacques Lanctot, Caramel and Cafee for their unconditional love and support. . . but also my cousin Farid, who recently purchased the kebab house "Ch'kiffEnCriss" across from "La Hacquiniere" RER B station. And finally, special thanks to Lucas, Matou, le Je, Kurimu, Ayoubou, and Johnny boy, who were always by my side even while overseas and across the equator.

Contents

Abstract	ii
Acknowledgements	iv
List of Figures	viii
1 Introduction	1
2 The Neurophysiology of Saccade Generation	3
2.1 Saccade generation: the neural basics	3
2.2 Gain Adaptation and its neural substrate	6
2.2.1 The Cerebellum	7
2.2.2 The Superior Colliculus	9
3 The Multiple Timescales of Memory: Evidence From Saccade Adaptation	12
3.1 Abstract	12
3.2 Introduction	13

CONTENTS

3.3	Materials and Methods	15
3.3.1	Experimental Setup	16
3.3.2	Experimental Paradigms	16
3.3.3	Data analysis	19
3.4	The System Identification Problem	19
3.5	Results	22
3.5.1	Effect of error-clamp trials	23
3.5.2	Effect of the 30sec break between sets	25
3.5.3	The multiple states of motor memory	26
3.6	Discussion	28
4	Saccade Dynamics Modeling: an Application of Control Theory	34
4.1	Model of the Saccadic Plant	35
4.2	Optimal Control	37
4.3	The Internal Value of a Goal	41
5	Gain-Adaptation Direction Engages Different Adaptive Mechanisms	45
5.1	Materials and Methods	46
5.1.1	Experimental Setup	46
5.1.2	Experimental Paradigm	47
5.1.3	Data Analysis	49
5.2	Results	50

CONTENTS

5.2.1	Saccade Kinematics	50
5.2.2	Saccade Latencies	53
5.3	Discussion	56
5.3.1	Forward model adaptation versus adaptation via target remapping .	56
5.3.2	Why latencies vary between groups and between conditions	61
5.3.3	Other related gain-adaptation saccade studies	63
5.4	Conclusion	64
	Vita	74

List of Figures

3.1	Experimental paradigm	18
3.2	Adaptation, extinction, and spontaneous recovery of saccade gains	24
3.3	Distribution of model parameters	28
4.1	Simulation of saccade profile for different target amplitudes	40
4.2	Shape of the cost function for different values of α	42
4.3	Simulation of saccade profile for different values of α	43
4.4	Sample of fatigue data	44
5.1	Trial-by-trial saccade characteristics for gain-down adaptation versus corresponding mimic-adaptation	51
5.2	Trial-by-trial saccade characteristics for gain-up adaptation versus corresponding mimic-adaptation	52
5.3	Bar plots for adaptation vs mimic-adaptation comparison	54
5.4	Saccade latency trial-by-trial and bar plot	55
5.5	Credit assignment as a function of target-jump size and direction	59
5.6	Saccade simulation for Gain-Down adaptation	60

Chapter 1

Introduction

Although there has been much research on saccade adaptation and its underlying neuromechanisms done in the past few decades, the phenomenon is still, from many perspectives, poorly understood. There is no consensus in the oculomotor scientific community on how changes of behavior are related to plasticity in the saccade circuitry, let alone more subtle points related to its temporal features, about its characteristic movement metrics, or about the interaction of different adapted states with each other. However, as is generally the case, more finely-defined questions are easier to tackle, and the approach here was to attempt to answer them with simple, easy to understand experimental paradigms and models.

The material in this essay covers three main projects, two of which are in published articles in the *Journal of Neurophysiology* and the *Journal of Neuroscience*. The last project is currently in the writing stage with the aim of an upcoming submission.

CHAPTER 1. INTRODUCTION

Chapter 2 surveys the basics of the neurophysiology of saccades. The role of different components of the saccadic circuitry in gain adaptation is then discussed with references to both physiological and behavioral research studies.

Chapter 3 goes over a study putting prolonged adaptation in competition with a sudden reverse-adaptation training. The results demonstrate that saccade adaptation is steered by two distinct memory systems. A model nicely reproduces the experimental data and gives insights about important features of these systems.

A model utilizing the principles of optimal control theory to rationalize the shape of the saccade speed profile and the sequence of motor commands used to generate it is then presented in chapter 4. An improvement that accounts for the changes in saccade kinematics is then added and the concept of "internal value" of a goal is introduced.

Finally, chapter 5 covers a comparative study between the saccade kinematics in a gain-adaptation paradigm versus in a control condition. The model expounded in the previous chapter is then used to gain a better understanding of the mechanisms underlying the differences in behavior.

Chapter 2

The Neurophysiology of Saccade Generation

2.1 Saccade generation: the neural basics

This section attempts to summarize the essential neuromechanisms and pathways involved in the generation of saccades in humans (cf. [1] for a more extensive review). Emphasis is put on the machinery underlying horizontal saccades as these are best understood and represent the main focus of the research presented in this thesis.

When a target signal appears in one's field of view, its luminosity excites the photoreceptors located at a precise point on the retina, thereby providing an estimate of the target's position in the 2D space. This signal is carried through V1 (also called the striate cortex or the primary visual cortex) and the extrastriate cortex located in the occipital lobe via the

CHAPTER 2. THE NEUROPHYSIOLOGY OF SACCADE GENERATION

lateral geniculate nucleus (LGN), in the thalamus. These activated areas are then relayed to various cortical areas of the brain for further visual information processing, motor planning and/or control. Namely, the most prominent of these areas are the Lateral IntraParietal area (LIP), the Frontal Eye Fields (FEF), and the Supplementary Eye Fields (SE). These signals next converge in the midbrain on the Superior Colliculus (SC), the main center involved in saccade generation. Projections from the SC are the main descending tract to the burst neurons located in the Brainstem Burst Generator (BBG) that directly send input to the motoneurons controlling the eye muscles. These burst neurons can intensify - in this case they are called the excitatory burst neurons (EBNs)- or curb - in that case, the inhibitory burst neurons (IBNs) - the activity of the motoneurons driving the extraocular muscles. SC is however not the only input to the BBG. There is a second pathway thought to be of crucial importance for the control of saccades. This pathway departs from the SC via the Nucleus Reticularis Tegmenti Pontis (NRTP) in the basal pons to regions in the cerebellum called the Oculomotor Vermis (OMV) (more specifically lobules VII and VIc of the posterior vermis) and the Caudal Fastigial Nucleus (cFN) [2, 3]. These two last regions finally project to the BBG (the OMV intermediately projects to cFN) and so exert an additional, thought to be modulatory, control on the extraocular muscles. This last region, the cFN, is often named the Fastigial Oculomotor Region (FOR) and will be referred to as such in the rest of this document. Finally, a third region, the FEF, is known to project to the BBG, but with a much smaller density of projections compared to the SC and cerebellum.

The burst neurons (both EBNs and IBNs) are among the lowest-level neural actors

CHAPTER 2. THE NEUROPHYSIOLOGY OF SACCADE GENERATION

involved in the generation of a saccade. Through motoneurons, they control the muscles responsible for horizontal saccadic eye movements, which are called the lateral rectus muscle (abduction movement when contracting) and the medial rectus muscle (adduction movement when contracting). The EBNs and the IBNs in a given side of the brain - say, the right - work in concert to trigger precise ipsilateral movements - movements to the right - aimed at a target in the periphery. In order to achieve this movement, EBNs send excitatory signals to the ipsilateral motoneurons driving the lateral rectus muscle of one eye. Meanwhile, the IBNs send inhibitory signals to the contralateral motoneurons driving the lateral rectus muscle of the other eye; hence triggering a saccade in the ipsilateral direction (with respect to the burst neurons). The onset of firing is about 10 msec before movement and lasts until near the end of ipsiversive saccades [4], also said to be the 'on-direction' of the neurons. This naming is explained by the fact that these burst neurons fire mainly for saccades aimed in that direction. This activity is thought to be the triggering signal that drives the saccades, or, in the other words, their initiating motor commands.

When a saccade is approaching its target goal, the burst neurons also act to prevent the eye from overshooting the target. Indeed, some of them also fire in their 'off-direction', their discharge being better timed with the end of the saccade. About half of IBNs [5] and some EBNs [6] discharge with contraversive saccades and act much like a brake would (to understand this, one can follow the opposite reasoning described above).

Thus, generating a saccade can approximately be thought of as the combination of two distinct mechanisms. One is triggering the saccade and giving it impetus and the second is

CHAPTER 2. THE NEUROPHYSIOLOGY OF SACCADE GENERATION

choking it off so that the fovea lands at the desired location in space. The basic, low-level neuromechanisms involved are well understood and simple. The ipsilateral burst neurons fire proportionally to the force exerted on the agonist muscles and then the contralateral burst neurons fire proportionally to the force exerted on the antagonist muscles (of course, the forces generated are the consequence of the firing, not the other way around). So, from the driver's seat point of view, five variables are at its disposition to control a horizontal saccade. It can control the accelerating phase by picking (1) a firing rate and (2) a duration of firing on the ipsilateral side and then control the decelerating phase by determining (3) a firing rate, (4) a duration of firing and (5) the time at which it begins firing on the contralateral side. This is, of course, only a rough approximation as it is well established that burst neurons do not fire in a pulse-step fashion like this, but rather in what is called a pulse-slide-step manner [1]. Nonetheless, reasoning along these lines is often employed in the literature to gain an intuitive sense of the impact on saccades of the spike activity of various saccade-related neurons.

2.2 Gain Adaptation and its neural substrate

Saccade adaptation would be more accurately called "target eccentricity perceived by the retina versus movement amplitude executed" adaptation. Typical saccade adaptation paradigms consist in looking at targets that jump while the saccade is on the fly, inducing a post-saccadic error that, in turn, necessitates a second corrective saccade. People - and

CHAPTER 2. THE NEUROPHYSIOLOGY OF SACCADE GENERATION

also monkeys for that matter - will eventually adapt to targets that consistently jump in a given direction with a given magnitude and progressively perform a first saccade closer to the final, post-jump position of the target. This behavior is termed 'gain adaptation', the word 'gain' referring to the ratio between the amplitude of a saccade aimed at a target and the initial target eccentricity perceived with respect to the fovea.

The neural correlates of this adaptation are still under debate and numerous neural recording experiments probing different parts of the saccadic circuitry are conducted every year. This section will glance over research findings identifying two important elements of the saccadic circuitry as crucial sites possibly responsible for the plasticity causing saccadic adaptation (see [7] for a thorough review).

2.2.1 The Cerebellum

Much attention has been given to the cerebellum as the possible neural substrate for saccade adaptation. The cerebellum has been traditionally considered as a main locus for motor adaptation in general and its hard-wired connection to the BBG makes it a good candidate for adaptation-related plasticity. Referring to the previous section, the cerebellar pathway projects mainly from the FOR, contralaterally to the burst neurons in the BBG [8], and receives its input primarily from the SC via two pathways, one direct and the other going through the OMV.

A first evidence that the cerebellum is of critical importance in adapting saccades comes from studies in cerebellar patients. [9] demonstrated that human patients with cerebellar

CHAPTER 2. THE NEUROPHYSIOLOGY OF SACCADE GENERATION

lesions tend to suffer from a saccadic dysmetria that does not resolve significantly with time; this suggests that a working cerebellum is needed in order to adapt saccades. This pathology was also observed in lesion studies in monkeys, where specific lesions in the FOR or the OMV induced dysmetric saccades that the rest of the saccadic circuitry proved unable to compensate [10, 11].

Cerebellum malfunctioning not only produces irreversible saccadic dysmetria, but also impairs the ability to perform saccade adaptation. When oculomotor muscles of one eye are surgically weakened and the good eye patched, normal monkeys adapt by sending stronger motor commands to both eyes, resulting in hypermetric movement in the good eye. When the patch is then switched onto the other eye, the hypermetria wanes gradually. [12] found that total ablation of the cerebellum in monkeys resulted in an hypermetria two to three times the amount of normal animals and, additionally, in the inability to reduce saccade size when the normal eye was subsequently patched. Partial ablation involving only the OMV and/or the FOR produced similar results.

Neural recordings also show that the cerebellar pathway is involved in saccadic adaptation. [13] recorded from neurons in the FOR and reported that consistent changes occurred with adaptation: the latency of the burst for ipsiversive saccades as well as the number of spikes associated with contraversive saccades became positively correlated with saccade size. Many neural recording studies like this one, however, fail to compare how these changes in neural response differ from a 'natural' reduction of amplitude (i.e. through a simple decrease in target eccentricity). [14] recently attempted to address this issue when

CHAPTER 2. THE NEUROPHYSIOLOGY OF SACCADE GENERATION

she monitored the activity of the IBNs in the BBG during gain-down adaptation and demonstrated that their pattern of firing differed significantly from the expected change one would record from normal amplitude reduction. There was speculation that this modulation was linked with changes witnessed in the FOR during gain-reduction adaptation.

Unequivocally, the cerebellar pathway is strongly involved in saccadic adaptation. However, it would be a mistake to consider the cerebellum as the unique locus from which the readjustment of motor commands during adaptation arises.

2.2.2 The Superior Colliculus

The SC, just like the cerebellum, projects contralaterally to the BNs in the brain stem. The neurons in the SC are grouped together in movement fields: the direction and amplitude of a saccade is encoded in a topographic map across the collicular surface. Therefore, unlike the BNs that discharge best for either the horizontal or vertical component of an eye movement, the neural commands in the superior colliculus are represented in vector coordinates [15].

There is evidence that at least part of the adaptation is occurring upstream of or in the superior colliculus. [16] found that after horizontal adaptation, only partial transfer (41%) to the horizontal component of post-training oblique saccades could be observed. If the horizontal component had been adapted separately from the vertical component, a 100% transfer should have been observed. Note that, nonetheless, the significant transfer (greater than 0%) also hints at the fact that some of the adaptation may occur downstream of a

CHAPTER 2. THE NEUROPHYSIOLOGY OF SACCADE GENERATION

vectorially-coded SC.

On the neural recording side, [17] recorded from neurons in the SC of rhesus monkeys during gain-down adaptation and found that their discharge was correlated more with the target location on the retina rather than with the post-adapted amplitude of the saccade; thereby arguing in favor of an adaptation site downstream of the SC. In fact, only 37% of the neurons showed that correlation (63% showed no correlation and no neuron the opposite correlation). For this reason and since the possibility that movement fields get shifted during adaptation can't be ruled out, their conclusions are much disputed. Furthermore, this data was challenged 10 years later by [18] when they determined that a significant change in response from the neurons in the SC occurred when monkeys adapted in the same task.

More evidence pointing to the SC as an adaptation site involves adapting electrically-elicited saccades. Saccades of the same direction and amplitude can be triggered by repeatedly stimulating an area in the SC of monkeys. It is then possible to adapt those saccades by displaying a target spot farther or short of their landing point. When a consistent error-signal is given, saccades start to adapt just like they do with normal targeting saccades [19]. Moreover, adaptation in electrically-elicited saccades can transfer, although partially, to targeting saccades. The question of the existence of the converse transfer has unfortunately produced inconclusive, conflicting results [19, 20]. These experiments indicate that adaptive changes are taking place somewhere downstream of or at the SC.

Considering the state of current research, it seems very unlikely that the SC is not in-

CHAPTER 2. THE NEUROPHYSIOLOGY OF SACCADE GENERATION

curing at least some of the plasticity that could account for saccadic adaptation. Therefore, any neuromimetic model or theory dismissing changes in this area of the brain is exposed to failure in describing the phenomenon neurally and should therefore be considered grossly approximate at best.

Finally, one should always keep in mind that the brain is an utterly complex system which contains about 100 billion neurons. An incredibly large number of neurons are involved in the saccadic circuitry, and, in the face of the small number each study is actually recording from, one should consider the results of these with reserve. The relationship between one neuron firing and the consequence seen at the other end of the saccadic system can become highly speculative. Moreover, there are many other putative mechanisms (other than the direct projections to the BNs) by which action potentials in the SC or the cerebellum can affect the way a saccade is generated. The existence of omnipause neurons (OPNs), a type of neuron playing an important role in controlling the saccadic system, is one example amongst many others that complicate the story to a great extent. That alone may be an important confound and should be kept in mind when hypothesizing about the role of various neural components ultimately projecting to the BBG.

Chapter 3

The Multiple Timescales of Memory: Evidence From Saccade Adaptation

This chapter was submitted as a paper that was subsequently published by the author in the *Journal of Neurophysiology* in 2008. It demonstrates how saccade adaptation can be thought of as a mechanism involving two distinct memory systems. Experimental evidence and an advanced analysis with linear two-state modeling constitute the core of the argument supporting this hypothesis.

3.1 Abstract

It is possible that motor adaptation in the timescales of minutes is supported by two distinct processes: one process that learns slowly from error but has strong retention, and an-

CHAPTER 3. THE MULTIPLE TIMESCALES OF MEMORY: EVIDENCE FROM SACCADE ADAPTATION

other that learns rapidly from error but has poor retention. This two-state model makes the prediction that if a period of adaptation is followed by a period of reverse-adaptation, then in the subsequent period in which errors are clamped to zero (error-clamp trials) there will be a spontaneous recovery, i.e., a rebound of behavior toward the initial level of adaptation. Here we tested and confirmed this prediction during double-step, on-axis, saccade adaptation. When people adapted their saccadic gain to a magnitude other than one (adaptation) and then the gain was rapidly reversed back to one (reverse-adaptation), in the subsequent error-clamp trials (visual target placed on the fovea after the saccade) the gain reverted toward the initially adapted value and then gradually reverted toward normal. We estimated that the fast system was about 20 times more sensitive to error than the slow system, but had a time constant of 28 seconds while the slow system had a time constant of nearly 8 minutes. Therefore, short-term adaptive mechanisms that maintain accuracy of saccades rely on a memory system that has characteristics of a multi-state process with a logarithmic distribution of timescales.

3.2 Introduction

The phenomenon of spontaneous recovery has been extensively observed in memory research, particularly in the classical conditioning paradigm [21]. In this paradigm, the animal is presented with a paired conditioned and unconditioned stimuli (CS and US) until the association is learned. Subsequently, the CS is presented without the US until it no

CHAPTER 3. THE MULTIPLE TIMESCALES OF MEMORY: EVIDENCE FROM SACCADE ADAPTATION

longer produces a response (termed extinction). Interestingly, in the post-extinction period the animal increasingly shows some of its previously learned response to the CS. In the literature on motor control, a similar phenomenon has been observed in control of eye movements: when monkeys adapt control of their saccades to an artificial manipulation of the target, and then are rapidly de-adapted back to the baseline state, subsequent passage of time in complete darkness (in which no errors are available) makes the oculomotor system revert back toward its initially adapted state [22].

Recently, we proposed that a simple model of memory can explain this general phenomenon [23]. In this model, learning is affected by two factors: prediction error, which causes the brain to adapt and change its behavior in order to minimize errors in subsequent trials, and passage of time, which causes forgetting. The model explained that in a typical short-term training paradigm (many minutes), behavior was supported by two processes: a fast adaptive process that was highly sensitive to error but had poor retention, and a slow adaptive process that had poor sensitivity to error but had robust retention. Behavior was the sum of these two processes. The model explained that spontaneous recovery occurred because a typical adaptation/reverse-adaptation protocol triggered a specific chain of events: during the initial long period of adaptation, most of the behavior became dependent on the slow adaptive process. Reverse-adaptation training forced behavior to return to baseline not through washing out of the learning, but by introducing a fast process that competed with the slow process. With passage of time after reverse-adaptation, the fast process faded, allowing an apparent recovery of the initial response.

CHAPTER 3. THE MULTIPLE TIMESCALES OF MEMORY: EVIDENCE FROM SACCADE ADAPTATION

To test the model, we needed a protocol to continuously assay the state of the learner's memory during the spontaneous recovery period. This is difficult, however, because the state of the learner can change because of errors that might occur on various trials and because of the passage of time from trial to trial. Theoretically, spontaneous recovery is best observed if passage of time is the only factor that influences behavior. Therefore, we needed a protocol in which behavior was recorded continuously while errors were eliminated in every trial. These error-clamp trials were recently introduced in the context of reaching [23, 24]. Here, we employed a similar approach in a saccade adaptation experiment to test whether behavior exhibited spontaneous recovery after adaptation/reverse-adaptation training.

3.3 Materials and Methods

Subjects were recruited from our medical school community. The experiments were composed of two complementary double-step adaptation paradigms, together lasting a total of 45 minutes. Group 1 subjects trained in a gain-down (decrease) paradigm and then in a gain-up (increase) paradigm until the gain returned to baseline (n=9, including authors DZ and RS). Group 2 subjects (n=8, including authors RS) trained in a gain-up paradigm and then in a gain-down paradigm. Four subjects participated in both groups. There was at least a break of one day between the two experiments. Subjects gave written consent and the protocol was approved by the Johns Hopkins Institutional Review Board.

3.3.1 Experimental Setup

The position of either the right or the left eye was measured with a magnetic-field search-coil system [25] using directional scleral annuli (Skalar Medical BV, Delft, Netherlands). Raw coil signals were filtered in hardware (90-Hz low-pass Butterworth), digitized (1,000 Hz), and saved on computer for later analysis. Targets were rear-projected using a mirror-controlled laser beam of 2mm-diameter projected onto a translucent screen located 1m in front of the subject with a 15° step-response of faster than 10ms. The room was otherwise dark. The head of the subjects was stabilized with a bite bar of dental impression material.

3.3.2 Experimental Paradigms

Saccadic adaptation was induced using the standard double-step paradigm [26]. The experiment began with a sequence of error-clamp trials, then adaptation trials, and concluded with another set of error-clamp trials, as illustrated in Fig.3.1.

Adaptation trials. Trials (Fig.3.1A) began with a fixation target. At a random time in the range of 500-1000ms, the fixation target was turned off and target T1 appeared at 15° horizontal. Once the eye began moving toward T1, T1 was displaced to T2. The displacement was either 5° away from (gain-up) or 5° closer to (gain-down) the initial fixation point. The jump was triggered near the onset of the eye movement, defined as the moment where the eye crossed a virtual 2° window placed around the fixation point (only

CHAPTER 3. THE MULTIPLE TIMESCALES OF MEMORY: EVIDENCE FROM SACCADE ADAPTATION

visible to the experimenter). Target T2 was maintained for 500ms, at which time the trial ended and T2 became the fixation point for the next trial in the opposite direction. Over time, subjects learned to make a saccade in response to T1 that was smaller (gain-down paradigm) or larger (gain-up paradigm). Each adaptation set consisted of 60 trials. The mean inter-trial time was 1250ms. Between sets, subjects received 30 seconds of rest, in which they were asked to close their eyes.

Error-clamp trials. Trials (Fig.3.1B) began with a fixation target. At a random time in the range of 500-1000ms, the fixation target was turned off and target T1 was displayed at 15° horizontal. Once the saccade began, T1 disappeared and at 500 or 800ms later (Groups 1 and 2, respectively) it reappeared at the position where the eye was located at 10ms prior (i.e., 490 or 790ms). In this way, first no and then a zero visual error was present after the saccade. Due to slight amplitude asymmetry between leftward and rightward saccade, occasionally a drift away from the center developed over time. We restrained eye position inside a +/-20-degree range by resetting the fixation point to +/-5 degrees whenever the eye landed out-of-bounds. The mean inter-trial time was 1250ms and 1550ms (for Groups 1 and 2, respectively).

Control trials. At the start of each experiment, subjects performed 20 trials in which the visual target at 15° horizontal remained present throughout the saccade and post-saccadic periods.

Group 1: Gain-down then gain-up. The sequence of trials is illustrated in Fig.3.1C. Subjects performed 180 error-clamp trials consisting of 90, 60 and then 30 trials. They then

CHAPTER 3. THE MULTIPLE TIMESCALES OF MEMORY: EVIDENCE FROM SACCADIC ADAPTATION

had 480 gain-down trials followed by 60 gain-up trials. The gain-up trials were followed by a sequence of 30, 60 and 90 error-clamp trials. A brief rest period (30 seconds) was inserted between sets as shown in Fig.3.1C.

Group 2: Gain-up then gain-down. For this group, the pattern of training was the same as in Group 1 except that gain-down training followed gain-up training.

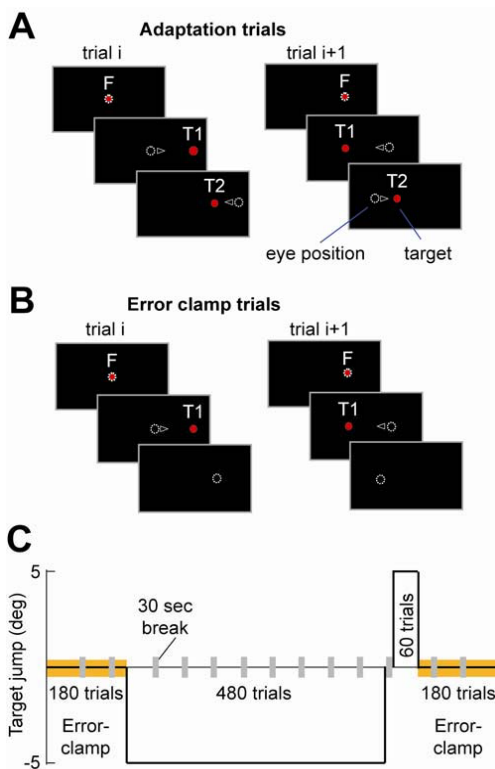


Figure 3.1: Experimental paradigm. **A.** Adaptation trials (gain-down shown here). **F:** fixation. **T1:** target of the saccade. **T2:** remapped target during the saccade. Small triangle: direction of eye movement. The trial ended with the eyes at **T2**, which then became the fixation for the next trial. **B.** Error-clamp trials. **T1** disappeared upon saccade initiation. After a brief period in the dark (500 or 800ms), it reappeared at the exact position of the fovea. That point became the fixation point for the next trial. **C.** The training sets began with 180 error-clamp trials, followed by 480 adaptation trials, 60 extinction trials, and finally 180 error-clamp trials. Adaptation for Group 1 was gain-down (as shown here) and for Group 2 was gain-up (not shown).

3.3.3 Data analysis

The duration of saccades was determined by a 20-deg/sec speed threshold. Discriminating criteria were used to dismiss abnormal saccades. Saccades were rejected (i) if they didn't reach a peak velocity higher than 90 deg/sec; (ii) if they had a latency less than 100ms; (iii) if they displayed multiple peaks in their speed profile; (iv) and finally if they were shorter than 50% of the target displacement. Most subjects had less than 5% of their saccades falling under one or more of these aforementioned criteria, with none of them exceeding 10% of all saccades.

3.4 The System Identification Problem

We assumed that the learner's behavior (saccade amplitude) on any given trial depended on the values of two hidden states (effectively, the states of the memory). We represent these states with vector \mathbf{x} (a 2x1). The states were affected by three factors: visual error \tilde{y} at end of a saccade, passage of time between trials, and Gaussian noise $\epsilon_{\mathbf{x}}$. If we assume that the inter-trial interval is constant, then we can write the change in states from trial to trial as:

$$\mathbf{x}^{n+1} = \mathbf{A}\mathbf{x}^n + \mathbf{b}\tilde{y}^n + \epsilon_{\mathbf{x}} \quad (3.1)$$

In this equation, the matrix \mathbf{A} (a diagonal 2x2) specifies how the states will change from trial n to $n+1$ because of passage of time, and the vector \mathbf{b} specifies how the states will change because of the error observed on trial n . We cannot directly observe the states,

CHAPTER 3. THE MULTIPLE TIMESCALES OF MEMORY: EVIDENCE FROM SACCADE ADAPTATION

but can measure saccade amplitude on trial n as y , which we assume is affected by target displacement p^n , some inherent bias that the subject may have y_b , a weighted sum of all memory states (the weights are unknown), plus execution noise ϵ_y . This is written as:

$$y^n = p^n - y_b + \mathbf{c}^T \mathbf{x}^n + \epsilon_y \quad (3.2)$$

In Eq.3.2, the vector \mathbf{c} specifies the relative weight of each state in influencing the saccade amplitude. Our next step is to transform these equations so that they can be easily fitted to our data (the sequence of saccade amplitudes y^n).

The error on trial n is due to the intra-saccadic displacement that we imposed on the target. If we write that displacement as u^n , then the error on that trial is:

$$\tilde{y}^n = p^n + u^n - y^n - y_b \quad (3.3)$$

$$= u^n - \mathbf{c}^T \mathbf{x}^n - \epsilon_y \quad (3.4)$$

Inserting Eq.3.4 into Eq.3.1 produces our state space model of the task:

$$\mathbf{x}^{n+1} = (\mathbf{A} - \mathbf{b}\mathbf{c}^T)\mathbf{x}^n + \mathbf{b}(u^n - \epsilon_y) + \epsilon_x \quad (3.5)$$

$$y^n = p^n - y_b + \mathbf{c}^T \mathbf{x}^n + \epsilon_y \quad (3.6)$$

In our experiment, for each subject we gave a sequence of targets p^n , displaced that target during the saccade by amount u^n , and measured the saccade amplitude y^n . In adaptation trials, u^n was the intra-saccadic target displacement. In error-clamp trials $u^n = y^n - p^n + y_b$

CHAPTER 3. THE MULTIPLE TIMESCALES OF MEMORY: EVIDENCE FROM SACCADE ADAPTATION

In summary, the mathematical problem consists in finding the parameters of the adaptive system of Eq.3.4, given a sequence of inputs u^n (target displacements) and measurements y^n (saccade amplitudes).

A recent breakthrough called sub-space identification [27] provides elegant, closed-form solutions for identification of stochastic linear systems. What we did in the above derivation is to transform our adaptive system equations into a form that can easily be solved by this approach. Once the parameters of the system are identified, we can estimate the state vector (i.e., the memory state) at each time step using a Kalman filter.

It is important to note that there is an infinite space of solutions to our problem, i.e., the same set of input and output data can be generated by an infinite number of systems that, from the point of view of Eq. 3.4, are indistinguishable. A particularly useful solution among these is one in which the matrix A is diagonal, assigning a unique time constant to each state. After estimation of the parameters, we transformed the system to one where A was diagonal. This produced a time constant of forgetting for each state. To interpret the time scales, we translated the state update equation of the discrete system of Eq. 3.4 to continuous time:

$$\dot{\mathbf{x}}(t) = A_c \mathbf{x}(t) + b_c u(t) + \pi_x \quad (3.7)$$

where $A_c = \Delta^{-1}(A - \mathbf{bc}^T - I)$, $b_c = \Delta^{-1}\mathbf{b}$, and Δ is the inter-trial interval, set to 1250ms. If we represent vector \mathbf{x} as $[x_f, x_s]^T$, i.e., the fast and slow states, then λ_s and λ_f refer to the time constant of the solution to this differential equation.

3.5 Results

We employed two kinds of trials in our experiments. In an adaptation trial, the visual target was displaced during the saccade (e.g., Fig.3.1A, gain-down training). In an error-clamp trial (Fig.3.1B), visual cues were removed at saccade onset and withheld until 500ms (Group 1) or 800ms (Group 2) after the saccade. At that time, the target was shown at precisely the current eye position. The idea was to assay the state of the saccadic system without introducing endpoint errors. The protocol consisted of the following blocks of trials: error-clamp, adaptation training, reverse-adaptation training, and error-clamp (Fig.3.1C).

Figs.3.2A and 3.2B show representative and average saccade amplitude data for the two groups. In Group 1, saccades were hypometric ($13.2^\circ \pm 0.47$, mean and SEM) in the initial set of error-clamp trials. The ensuing gain-down adaptation induced a rapid decrease in amplitude in the first set, followed by a slower decrease in the seven remaining sets. By the last set of gain-down training, saccade amplitude had dropped to $10.0^\circ \pm 0.32$. It took only 60 trials in the following gain-up training to bring the saccade amplitudes to near baseline ($13.0^\circ \pm 0.30$ for the last six trials). However, in the subsequent error-clamp trials saccade amplitudes did not remain stationary. Rather, they sharply declined ($p = 0.002$, one-sided t-test, within-subject comparison of the last six trials of gain-up vs. last six-trials of the immediately following the set of error-clamp trials). In the last two sets of the error-clamp trials amplitudes were $11.4^\circ \pm 0.52$ ($p < 0.0001$, one-sided t-test, within subject comparison of first and last two sets of error-clamp trials). Therefore, when gain-down training was followed by a rapid period of gain-up training, in the following

CHAPTER 3. THE MULTIPLE TIMESCALES OF MEMORY: EVIDENCE FROM SACCADE ADAPTATION

error-clamp trials the amplitudes reverted back toward the values achieved in the initial gain-down period.

We observed a similar pattern of spontaneous recovery when gain-up training was followed by gain-down training (Group 2, Fig.3.2B). In the initial error-clamp trials saccades were hypometric ($12.9^\circ \pm 0.51$). Amplitudes increased rapidly in the initial gain-up set and then gradually increased to $16.0^\circ \pm 0.41$ by the final set. The 60 trials of reverse-adaptation training were sufficient to rapidly reduce saccade amplitudes to slightly below baseline levels ($12.1^\circ \pm 0.51$ by the last six trials of the gain-down training). In the subsequent error-clamp trials, however, saccade amplitudes sharply increased ($p = 0.004$ one-sided t-test, within subject comparison of the last six trials of gain-down vs. last six-trials of the immediately following error-clamp trials). Amplitudes remained significantly larger than baseline in the final two error-clamp trials ($13.8^\circ \pm 0.56$, $p = 0.003$, one-sided t-test, within subject comparison of first and last two sets of error-clamp trials). In summary, when adaptation was followed by a rapid period of reverse-adaptation training, in the following period of error-clamp trials saccade amplitude continued to change, reverting toward the behavior exhibited during initial adaptation.

3.5.1 Effect of error-clamp trials

Saccades in the initial error-clamp trials were hypometric, as is typical for saccades made in the dark to single sources of light [28]. However, no visual feedback was available in error-clamp trials for 500-800ms. Did this delay in feedback influence saccade

CHAPTER 3. THE MULTIPLE TIMESCALES OF MEMORY: EVIDENCE FROM SACCADIC ADAPTATION

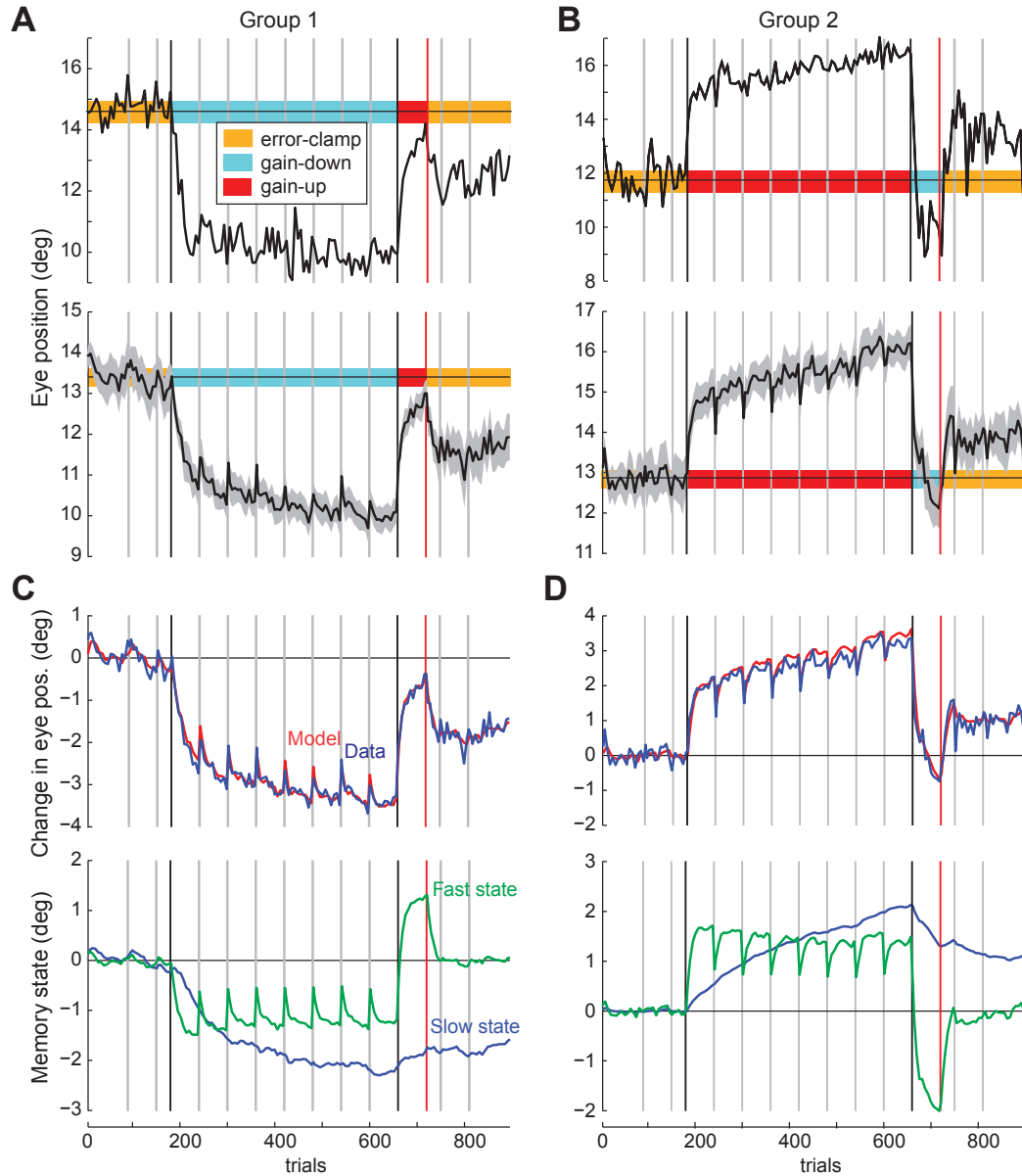


Figure 3.2: Adaptation, extinction, and spontaneous recovery of saccade gains. In all plots, the vertical gray lines indicate 30 second set breaks. The two vertical black lines mark the beginning and end of the adaptation trials. The vertical red line marks the end of the extinction trials. **A** and **B**. Representative saccade amplitudes and group data (with SEM). Data was averaged using variable bin widths to show the rapid changes that occur at set breaks: In each set, the bin size was two trials for the first bin, then four trials, then six trials for all subsequent bins for that set. **C** and **D**. The top sub-plot shows the fit of Eq.3.4 to the mean data. The bottom plot shows the contribution of each hidden state to the motor output. The bin sizes are the same as parts **A** and **B**.

CHAPTER 3. THE MULTIPLE TIMESCALES OF MEMORY: EVIDENCE FROM SACCADE ADAPTATION

amplitudes? A recent report suggests that for large saccades ($22^\circ - 34^\circ$), lack of visual feedback at saccade termination may result in an increase in saccade amplitudes [29]. To check for this, we compared the amplitudes of saccades in the initial sets of error-clamp trials to a set of control saccades immediately preceding these trials: Before the main experiment began, subjects in both groups performed 20 trials in which the visual target at 15° remained lit throughout the saccade and post-saccade inter-trial periods. For Group 1, amplitudes in the control period ($13.3^\circ \pm 0.13$) were indistinguishable from the amplitudes in the following error-clamp trials ($13.2^\circ \pm 0.47$, t-test $p > 0.5$). To examine this question further, we increased the delay period in Group 2 to 800ms from the value of 500ms in Group 1. Similar to Group 1, amplitudes in the control period in Group 2 ($13.3^\circ \pm 0.24$) were not reliably distinguishable from the amplitudes in the following error-clamp trials ($12.9^\circ \pm 0.51$, $p > 0.1$). Therefore, error-clamp trials did not appear to significantly bias the amplitudes of saccades.

3.5.2 Effect of the 30sec break between sets

The group data shown in Figs. 3.2A and 3.2B suggests that the brief set breaks might have had a highly repeatable effect on saccade amplitudes. That is, in Group 1 the set breaks appeared to coincide with an increase in the amplitudes during the gain-down adaptation blocks, whereas in Group 2 the set breaks coincided with a decrease in the amplitudes during the gain-up adaptation blocks. To quantify this effect, for each subject we compared the last four saccades in each set with the first four saccades in the following set during the

CHAPTER 3. THE MULTIPLE TIMESCALES OF MEMORY: EVIDENCE FROM SACCADE ADAPTATION

gain-down trials in Group 1 and gain-up trials in Group 2. On average, subjects in Group 1 showed an increase of $0.6^\circ \pm 0.17$ ($F(7,1)=14.9$, $p < 0.01$) and subjects in Group 2 showed a decrease of $0.6^\circ \pm 0.21$ ($F(8,1)=7.84$, $p < 0.05$) during the set breaks. Therefore, the 30sec breaks between sets produced a significant forgetting. The amount of forgetting was indistinguishable between the two groups.

3.5.3 The multiple states of motor memory

Spontaneous recovery is a signature of an adaptive system that is supported by multiple states, each learning at a different timescale [23, 30]. To estimate these states and their timescales, we fitted the group data to a linear stochastic state-space model of learning (Eq.3.4). In this system, the motor output (saccade amplitude) was supported by two hidden states. The changes in these states were a function of time between trials and endpoint errors observed on each trial.

Figs. 3.2C and 3.2D show the fit of the model and plot the estimated contribution of each state to motor output, i.e., $\mathbf{c}^T \mathbf{x} = c_s x_s + c_f + x_f$, in which the subscripts denote the slow and fast states. In the initial error-clamp trials, both states were near zero and were driven only by noise. In the subsequent adaptation stage, the fast state learned rapidly while the slow state lagged behind. During the subsequent 30sec rest period between sets, the fast state showed a large decay while the slow state showed little or no decay. This model exhibited two fundamental properties of memory: a fast system that learned quickly but showed poor retention with passage of time, and a slow system that learned slowly but

CHAPTER 3. THE MULTIPLE TIMESCALES OF MEMORY: EVIDENCE FROM SACCADE ADAPTATION

had significantly better retention.

As the adaptation trials continued, the slow state overtook the fast state so that the by the end of gain-down training in Group 1 or gain-up training in Group 2, the slow states contribution was twice the fast state. Therefore, by the end of 480 adaptation trials (just before start of reverse-adaptation block) performance was dominated by the slow state.

In the subsequent set break, the fast state once again decayed toward baseline. However, in the subsequent training block (reverse-adaptation training) the errors were in the opposite direction of the previous training, forcing the fast state to rapidly learn and acquire values that now competed with the values of the slow state. By the end of the reverse-adaptation block, the sum of the two states was near baseline (top sub-plot of Fig. 3.2C, line labeled 'Model'), but of course the two states had not returned to baseline. In the following error-clamp trials (note that there was no set break here), the fast state rapidly declined to baseline whereas the slow state gradually declined. The sum effect was spontaneous recovery. That is, in Group 1 motor output reverted back toward the gain-down pattern and in Group 2 it reverted back toward the gain-down pattern.

The fit to the group data produced a decay time constant of $\lambda_f = 28sec$ for the fast state and $\lambda_s = 7min$ for the slow state. Error sensitivity of the fast state was 18 times larger for the fast state, i.e., $b_f/b_s = 18$. Finally, saccade amplitudes relied almost twice as much on the slow than the fast state, i.e., $c_s/c_f = 1.7$.

We next examined the distribution of these estimates by fitting the model to each subject and condition. The fit was satisfactory in 14 of 17 subjects and their parameter values are

CHAPTER 3. THE MULTIPLE TIMESCALES OF MEMORY: EVIDENCE FROM SACCADÉ ADAPTATION

plotted in Fig. 3.3. The data for the three subjects that we could not fit exhibited large variability in saccade amplitudes during the initial error-clamp trials. For the remaining 14 subjects, we found that $\lambda_f = 28 \pm 7 \text{sec}$ (mean $\pm 95\%$ CI), $\lambda_s = 7.8 \pm 3 \text{min}$, $b_f/b_s = 18 \pm 6$, and $c_s/c_f = 1.7 \pm 0.5$. Therefore, the time scales of the fast and the slow system, as well as their sensitivity to error, were an order of magnitude apart.

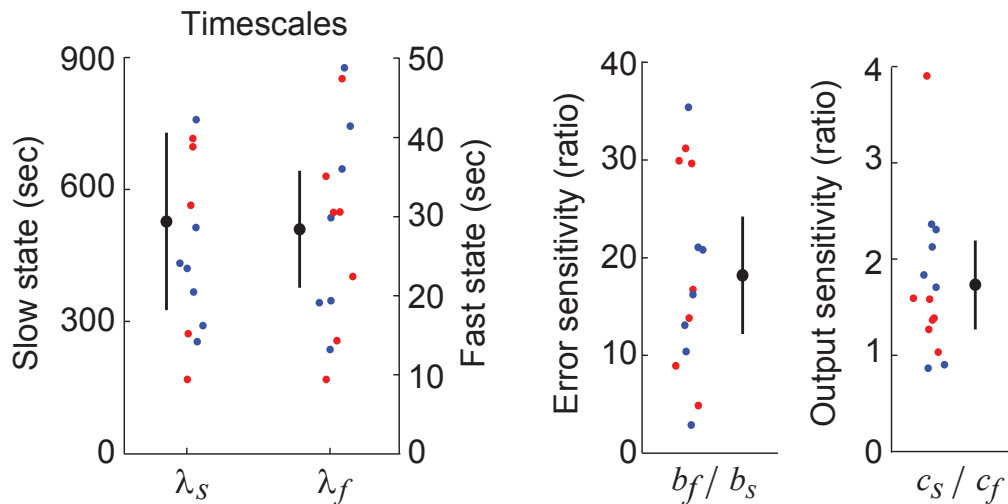


Figure 3.3: Distribution of model parameters when Eq.3.4 was fitted to each subject data. λ_s and λ_f are the time constants of the slow and fast states, which describe the sensitivity of these states to passage of time. b_s and b_f are the sensitivity of the two states to error. c_f and c_s are the weighted contribution of these states to the measured behavior.

3.6 Discussion

We tested the idea that the memory that contributes to the accuracy of saccades is composed of two functional states: a fast state that learns from error but has poor retention,

CHAPTER 3. THE MULTIPLE TIMESCALES OF MEMORY: EVIDENCE FROM SACCADE ADAPTATION

and a slow state that learns less from the same error but has better retention. The theory predicted that when adaptation is followed by reverse-adaptation, the resulting behavior will show spontaneous recovery of the initially acquired adapted state. To test for this, we began with an adaptation block that used intra-saccadic manipulation of the visual target to introduce endpoint errors. This was followed by a reverse-adaptation block in which the direction of the intra-saccadic target motion was reversed until the saccade amplitudes reached baseline. We then introduced error-clamp trials in which the post-saccadic visual information was withheld for 500 or 800ms, and then shown at the current eye position, signaling zero errors. Saccade amplitudes during this period of error-clamp trials exhibited spontaneous recovery, reverting back toward their initially adapted state.

Is there evidence that in short-term paradigms (up to 1 hour) the memory that supports generation of saccades is affected by both the passage of time and errors? [31] reported that when a block of gain-down adaptation trials (in which the target was moved intra-saccadically and remained visible in the post-saccadic period) was followed by trials in which the post-saccadic target was turned off, the reduced saccade amplitudes caused by gain-down adaptation gradually returned back to baseline. Therefore, passage of time produced a decay in the memory acquired during adaptation. However, the return to baseline was faster if the target remained stationary and the endpoint errors encouraged extinction. This is consistent with a model in which both error and passage of time affect the state of the learner.

If the saccades of the learner are supported by a memory that can be represented as a

CHAPTER 3. THE MULTIPLE TIMESCALES OF MEMORY: EVIDENCE FROM SACCADE ADAPTATION

single state, then adaptation followed by extinction will not produce spontaneous recovery [23]. Rather, in the post-extinction period saccade amplitudes simply return to baseline. However, if memory is effectively supported by two or more states, then the differential sensitivity of the purported states to error and passage of time can produce spontaneous recovery. That is, in trials in which errors are eliminated, the fast state should rapidly return to baseline, leaving behavior that reflects the slow state. Indeed, in the 30 error-clamp trials post extinction we observed a near 50% recovery of the saccade amplitudes. We estimated that during these trials the learning from the fast state had completely dissipated.

We found that during the 30sec break that separated each adaptation set, saccade amplitudes changed by about 0.6° with a direction that was opposite to the direction of adaptation. The model explained that this forgetting was due to the same fast process that produced spontaneous recovery in the post-extinction error-clamp trials. Therefore, it was crucial not to introduce a break between the extinction block and the error-clamp block. Such a break would prevent us from observing the rapid post-extinction change in saccade amplitudes.

How accurate is our assumption that error-clamp trials eliminated the error signal? The errors that drive saccade adaptation are derived mainly from visual information during the post-saccade period [16, 32]. When this information is delayed, the resulting adaptation is reduced or eliminated. For example, a 750ms delay reduces the error-dependent adaptive response by 90% [33]. In our paradigm, we not only included a delay in presenting the post-saccadic visual information, but we also presented the visual target at the current

CHAPTER 3. THE MULTIPLE TIMESCALES OF MEMORY: EVIDENCE FROM SACCADE ADAPTATION

eye position. Therefore, the combined techniques should reduce any error-driven adaptive response in a given trial even further.

Because saccades in the dark are hypometric, it is conceivable that when a post-saccadic target appears at the current eye position the brain interprets this as an error and attempts to reduce amplitude of the subsequent saccade. This would predict that error-clamp trials should increase hypometria. We checked for this by comparing saccade amplitudes in response to targets that did not disappear (control trials before start of the error-clamp trials) vs. targets that disappeared and then were shown after a delay at the current eye position (error-clamp trials) and did not find a significant difference. If error-clamp trials introduced inadvertent errors, the effect must be quite small because the same model that assumed zero-error in error-clamp trials and accounted for spontaneous recovery also explained the forgetting during the 30sec rest periods during which subjects were in complete darkness.

Perhaps the most significant contribution of the model is that it suggests the possibility that even in brief adaptation experiments, changes in behavior are not only a function of error, but also passage of time. The initially rapid and then gradual changes in the post-extinction trials are largely due to the effect of time passage on the states that supported the memory during error-dependent adaptation. The model predicts that functionally, these states have both fast and slow timescales, with values that are an order of magnitude apart. An order of magnitude also differentiates the sensitivities that these memory states express with respect to error. If one imagines that there are not two but many more states that support a memory, and their sensitivity to passage of time and error is distributed along a

CHAPTER 3. THE MULTIPLE TIMESCALES OF MEMORY: EVIDENCE FROM SACCADE ADAPTATION

logarithmic scale, then such models may be able to account for saccade adaptation data on timescales of weeks and months [30]. Therefore, such motor memory becomes 'cemented' only if it is repeated, causing adaptation in the slowest of the slow states.

The adaptive behavior that we examined here is grossly impaired when there is damage to the oculomotor vermis in the cerebellar cortex [34, 35] or fastigial oculomotor region in the cerebellar deep nuclei [36]. In other cerebellar-dependent paradigms it has been hypothesized that the initially rapid changes in behavior during adaptation may be due to changes in the cerebellar cortex, while the retention of the memory over the long-term (days) may depend on the cerebellar nuclei [37–39]. Of course, saccade adaptation may also engage structures other than the cerebellum. Therefore, one possibility is that the two timescales reflect changes in distinct anatomical substrates that all contribute to the motor commands that move the eyes.

This line of thinking would be bolstered if there was evidence for the two states in the trajectory of saccades. In a recent examination of cross-axis adaptation, we indeed found that the commands that initiated the saccade adapted more slowly than commands that arrived later in the same saccade [40]. For example, the 30sec break between sets produced dramatic forgetting in the late-acting motor commands, yet it had essentially no effect on the motor commands that initiated the saccade. If the late acting motor commands can be attributed to a 'steering' mechanism of the eyes via the cerebellum [14], then it is possible that the fast states are a reflection of a changing contribution from this structure.

However, the fact that we have observed two functional states of memory in no way im-

CHAPTER 3. THE MULTIPLE TIMESCALES OF MEMORY: EVIDENCE FROM SACCADE ADAPTATION

plies involvement of two distinct neural structures. In principle, the two states may reflect mechanisms of plasticity in a single neuron. From the point of view of the two-state model, spontaneous recovery is closely related to 'savings': when adaptation is followed by extinction, subjects exhibit faster relearning in a subsequent re-adaptation block. The two-state model explains both phenomena using the concept of fast and slow systems [23]. Recently, [41] demonstrated that behavioral changes during adaptation, extinction, and savings in a classical conditioning task that lasted about 16 hours were correlated with discharge of single Purkinje cells in the cerebellar cortex. Therefore, the multiple states that produced savings in that paradigm did not appear to require two or more distinct neural substrates, but were perhaps part of the molecular machinery that supported synaptic plasticity in single Purkinje cells.

Chapter 4

Saccade Dynamics Modeling: an Application of Control Theory

In striving to gain a better understanding of the whys and hows of saccade adaptation, mathematical modeling can be a very handy tool to conceptualize new hypotheses. This chapter presents a model of saccade generation taking advantage of a recently developed stochastic control theory algorithm [42]. The adaptation of the mathematical framework to propose a model of how saccades can be controlled was first developed by Dr. Haiyin Chen-Harris and later refined by the author. The model in its final version has been included in a co-authored, recently published paper in the *Journal for Neuroscience* [40].

4.1 Model of the Saccadic Plant

The oculomotor plant can be approximated by a simple second-order system composed of springs and dampings, representing the stiffness of the extraocular muscles and the viscosity inherent to an eye movement in its fluid-bathing socket, respectively. Let us consider movements in only one direction x . Newton's Second Law implies that:

$$m\ddot{x} = -kx - b\dot{x} + u \quad (4.1)$$

where m is the mass of the eyeball, k is the stiffness constant, b is the viscosity constant and finally u represents the forces exerted on the eye ball, which are generated by the aggregate neural commands sent by the saccadic system.

Transforming this second-order differential equation into its equivalent form of a system of two first-order differential equations, we get:

$$\underbrace{\begin{bmatrix} \dot{x}_1 \\ \dot{x}_2 \end{bmatrix}}_{\dot{\mathbf{x}}} = \underbrace{\begin{bmatrix} 0 & 1 \\ -k/m & b/m \end{bmatrix}}_{A_c} \underbrace{\begin{bmatrix} x_1 \\ x_2 \end{bmatrix}}_{\mathbf{x}} + \underbrace{\begin{bmatrix} 0 & 0 \\ 0 & 1/m \end{bmatrix}}_{B_c} \underbrace{\begin{bmatrix} 0 \\ u \end{bmatrix}}_{\mathbf{u}} \quad (4.2)$$

where $x_1 \equiv x$ and $x_2 \equiv \dot{x}$. The impulse response of such a system is characterized with a double-exponential relaxation toward the initial state ($x_1 = 0, x_2 = 0$). The time constants pertaining to the two exponentials can be related to the system's constants k , b , and m by performing the Laplace analysis of the impulse response in Eq.4.1. Doing so, we get the following results:

CHAPTER 4. SACCADE DYNAMICS MODELING

$$-\frac{k}{m} = -\frac{1}{\tau_1\tau_2} \quad ; \quad -\frac{b}{m} = -\frac{\tau_1 + \tau_2}{\tau_1\tau_2} \quad (4.3)$$

where τ_1 and τ_2 are the timescales of the two exponential decays. The time scales that are generally used in the field can be found in [43] and are $\tau_1 = 224ms$ and $\tau_2 = 13ms$. (However, these constants in fact refer to an older paper studying vergence in monkeys [44] and it is possible that they are either outdated and/or inaccurate and/or irrelevant for the human oculomotor system. The oculomotor modeling community would find it to be of great use to have a set of new data determining these constants with greater precision (e.g. cadaver studies, model fitting of large data sets, etc.)).

This continuous-time model can be transformed into a discrete-time model, which is much more convenient for computer simulations. To do this, we can use these exact (when no noise is considered) relationships between the continuous-time and discrete-time system matrices:

$$A_d = \exp(A_c\Delta)$$
$$B_d = A_c^{-1}(\exp(A_c\Delta) - I)B_c$$

where Δ is the time increment between each iteration.

Moreover, in reality the motor commands that are sent to the oculomotor plant are noisy. One distinctive characteristic of biological systems is that this noise is signal-dependent. Intuitively, this means that the higher in magnitude the intended motor commands are, the

CHAPTER 4. SACCADE DYNAMICS MODELING

more variable they are likely to be. This can translated in mathematical terms like so:

$$\mathbf{u}_{eff} := \mathbf{u} + \sum_n C_n \mathbf{u} \phi_n \quad (4.4)$$

where $\phi_n \sim N(0, 1)$, n goes from 1 to the size of vector \mathbf{u} , and C_n is a square matrix with elements $c_{ij} = \xi_n$ if $i = j = n$ and $c_{ij} = 0$ otherwise. Finally, ξ_n is a proportionality constant that determines the extent to which the n^{th} component of \mathbf{u} is sensitive to noise.

For reasons that will become evident later, we also wish the include the target position relative to the fovea r into the eye vector \mathbf{x} so that $\mathbf{x} = [x, \dot{x}, r]$; the system matrices will of course need to be modified accordingly. The complete second-order model of the oculomotor plant and its relationship to the motor commands that are being sent out can be summarized by one single equation (for simplicity $A \equiv A_d$ and $B \equiv B_d$):

$$\boxed{\mathbf{x}_{t+1} = A\mathbf{x}_t + B\mathbf{u}_t + B\sum_n C_n \mathbf{u}_t \phi_n} \quad (4.5)$$

Eq.5.2 can naturally be adapted to models with more than one degree of freedom, provided that we know the time constants of the impulse response in each of the additional directions.

4.2 Optimal Control

In order to reach its target r , the nervous system must send motor commands to the eye muscles. However, there are some constraints that need to be respected. First, we make the hypothesis that the nervous system does not want to waste energy and thus tries

CHAPTER 4. SACCADE DYNAMICS MODELING

to minimize the total amount spent to reach the desired target. Second, while the eye is moving, the subject is considered to be effectively blind. This can be interpreted as a cost for the eye to be in movement. We suggest that there is a duration range within which the brain accepts this momentary lapse in vision and after which the cost for not being at the target becomes critically detrimental. The constraints of arriving as soon as possible and minimizing the energy cost are summarized by a so-called cost-to-go function J that will be minimized:

$$J = \sum_t \mathbf{x}_t^T Q_t \mathbf{x}_t + \mathbf{u}_t^T R \mathbf{u}_t \quad (4.6)$$

Each term represents the cost to make an action at time t . R is a constant times the identity matrix and Q_t constructed so that:

$$\mathbf{x}_t^T Q_t \mathbf{x}_t = (x_t - r)q_{1,t}(x_t - r) + \dot{x}_t q_{2,t} \dot{x}_t. \quad (4.7)$$

where $q_{1,t} = q_1 H(t - \tau)$, $q_{2,t} = q_2 H(t - \tau)$, and $H(t)$ is the Heaviside step function. In other words, the first term in the summation starts penalizing for not being on target and for still being in movement after time τ . The reason r was included in the state vector \mathbf{x} should now become clear. The second term in Eq.4.6 expresses the concept that, at each time step, producing small motor commands is favored over bigger ones (minimum effort principle).

In this framework, $\{\{\xi_n\}, q_1, q_2, R\}$ are user-defined constants. The last constant τ , however, represents the desired duration of the movement and is optimized through a trade-off between the total cost of movement and a novel concept coined the "internal value" of

CHAPTER 4. SACCADE DYNAMICS MODELING

a movement. For now, though, we will assume that τ is known and determine the so-called control policy that dictates the values of \mathbf{u}_t at each time step.

[42] showed that for a system that has linear dynamics with signal-dependent noise the optimal choice for \mathbf{u}_t , the one that minimizes the total cost to arrive on target, could be expressed as a linear function of the current state vector \mathbf{x}_t :

$$\boxed{\mathbf{u}_t = -G_t \mathbf{x}_t} \quad (4.8)$$

where G_t is a gain that is calculated off-line, prior to the start of the movement, and recursively backward in time:

$$\begin{aligned} G_t &= (R + \Sigma_n C_n^T B^T W_x^{t+1} B C_n + \Sigma_n C_n^T B^T W_e^{t+1} B C_n + B^T W_x^{t+1} B)^{-1} B^T W_x^{t+1} A \\ W_x^t &= Q_t + A^T W_x^{t+1} A - A^T W_x^{t+1} B G_t \\ W_e^t &= A^T W_x^t + 1 B G^t + A^T W_e^{t+1} A \end{aligned}$$

The sequence of gains G_t then applied in Eq.4.8 lets us determine what is the 'best' motor command to give, given the current eye position, speed, and target position (all contained in \mathbf{x}_t). In practice, a system might have access to an estimate of \mathbf{x}_t instead of its true value, and use it to determine the next motor command. In this case, \mathbf{x}_t is replaced with its estimate $\hat{\mathbf{x}}_t$. How to form this estimate is a crucial question that implies the existence of a forward model and will be discussed in the next chapter.

CHAPTER 4. SACCADE DYNAMICS MODELING

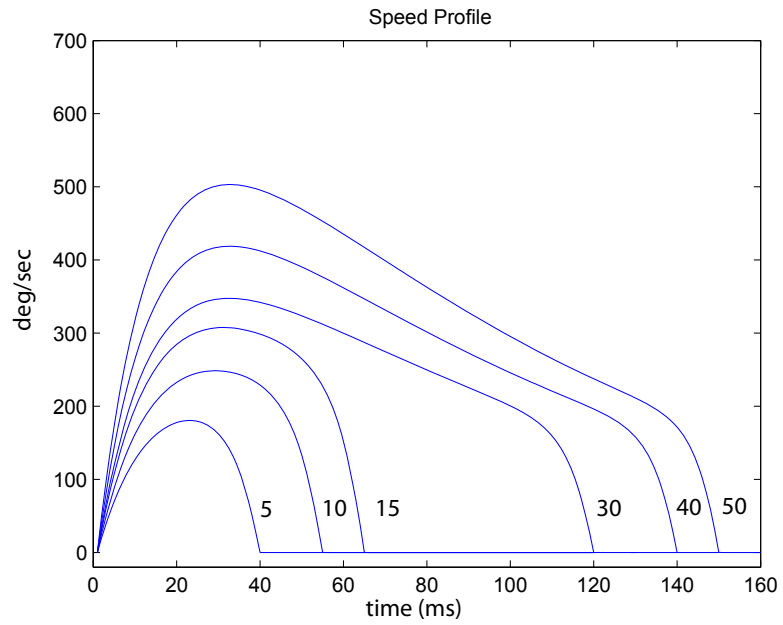


Figure 4.1: Saccade profile simulation for different amplitudes. α is constant.

parameters	τ_1 (ms)	τ_2 (ms)	R	q_1	q_2	ξ
values	224	13	1	10^4	10^4	0.02

Table 4.1: Simulation parameters used for Fig.4.1

4.3 The Internal Value of a Goal

The previous section demonstrated how to find the optimal motor command to reach a target given a desired duration τ . We propose here that τ is in fact determined so as to minimize a trade-off between the total cost of the movement and a separate cost for the duration:

$$J_\tau = \sum_{t=0}^{t=\tau} E[J_t] + \alpha\tau^2 \quad (4.9)$$

This new added quadratic cost $\alpha\tau^2$ gives a rationale that prohibits excessively long duration. Indeed, the first term in Eq.4.9 decreases as τ increases since the controller need not as high motor commands to reach the target on time, but the second term behaves inversely. Fig.4.2 shows that Eq.4.9 possesses a unique minimum that is approximately quadratic in τ around its neighborhood.

α is a constant representing how averse the system is to perform long movements. The higher the value of α , the smaller the optimal τ will be. This new parameter helps to conceptualize relatively vague ideas related to motivation, attention, or reward. In some sense, it encapsulates the idea of the internal value of a goal; or, in other words, how much value is there in reaching a target?

In particular, this concept allows us to explain a consistent and reproducible phenomenon observed in research on eye movements: when the eye makes repetitive saccades to the same targets, the movements tend to get slower and last longer, the amplitude re-

CHAPTER 4. SACCADE DYNAMICS MODELING

maintaining constant (see Fig.4.4). This 'fatigue' that occurs across time can be perceived as a reflection of a decrease in the internal value of the repeatedly reached goal. Indeed, as α decreases, the second term in Eq.4.9 gets weighted less, and, as a result, the new optimal τ causes the saccade to last longer. Fig.4.3 demonstrates how the model reproduces the fatigue behavior by changing the value of the goal α .

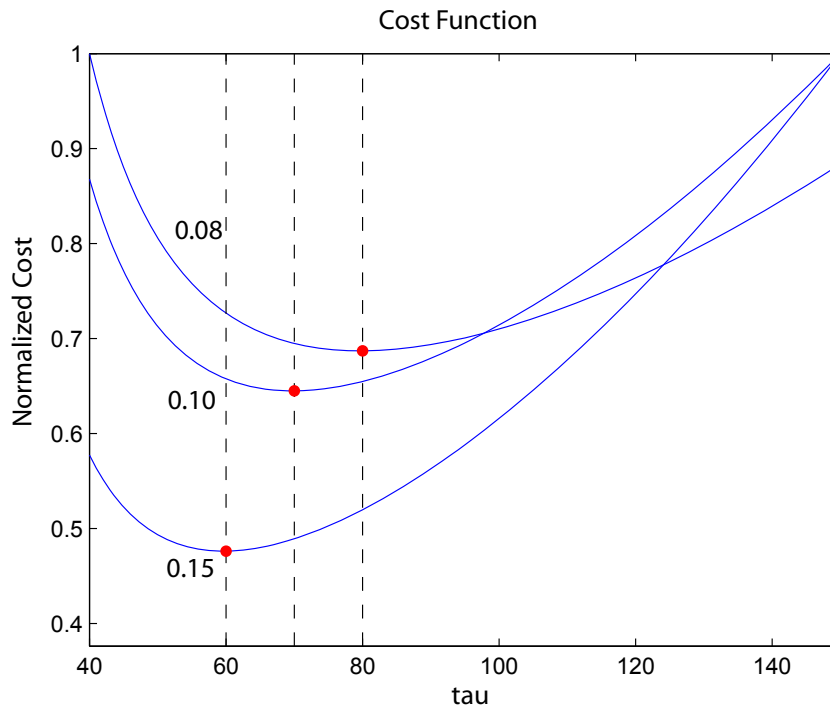


Figure 4.2: Shape of the cost function for different values of α . When the value α of the goal is high, the minimum is at a shorter desired duration τ . When $\alpha = 0.15$, the minimum duration is around $\tau = 60ms$. When $\alpha = 0.10$, $\tau = 70ms$ and when $\alpha = 0.08$ the minimum duration is close to $\tau = 80ms$

CHAPTER 4. SACCADE DYNAMICS MODELING

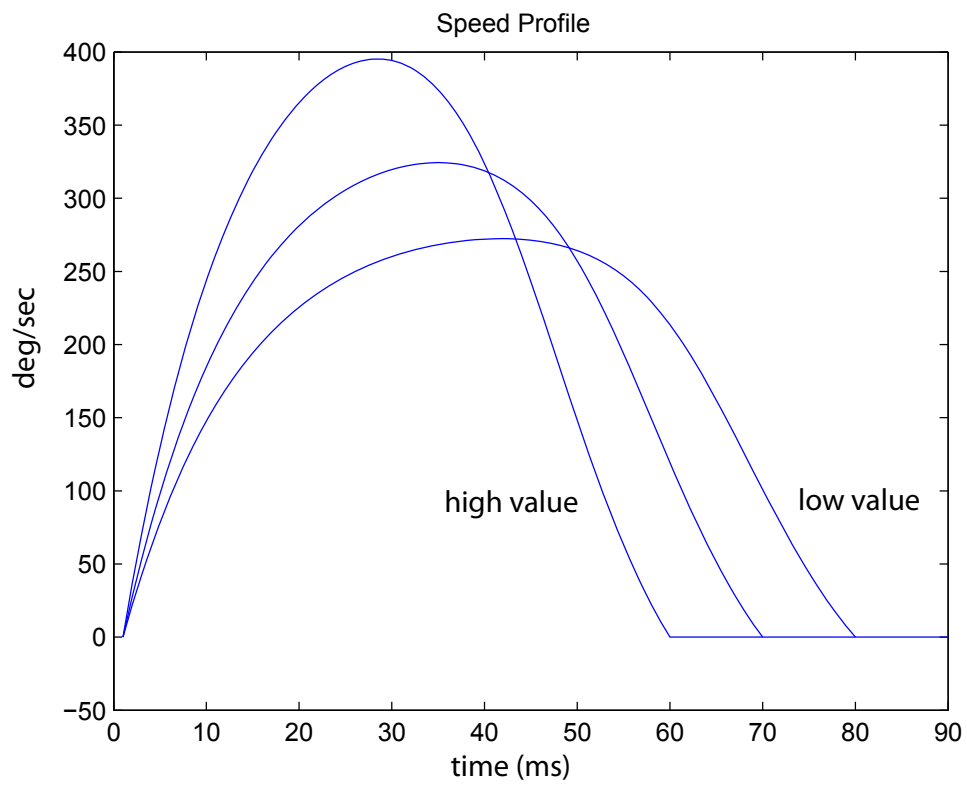


Figure 4.3: Simulation of saccade profiles for different values of α . Target is at 15° .

CHAPTER 4. SACCADE DYNAMICS MODELING

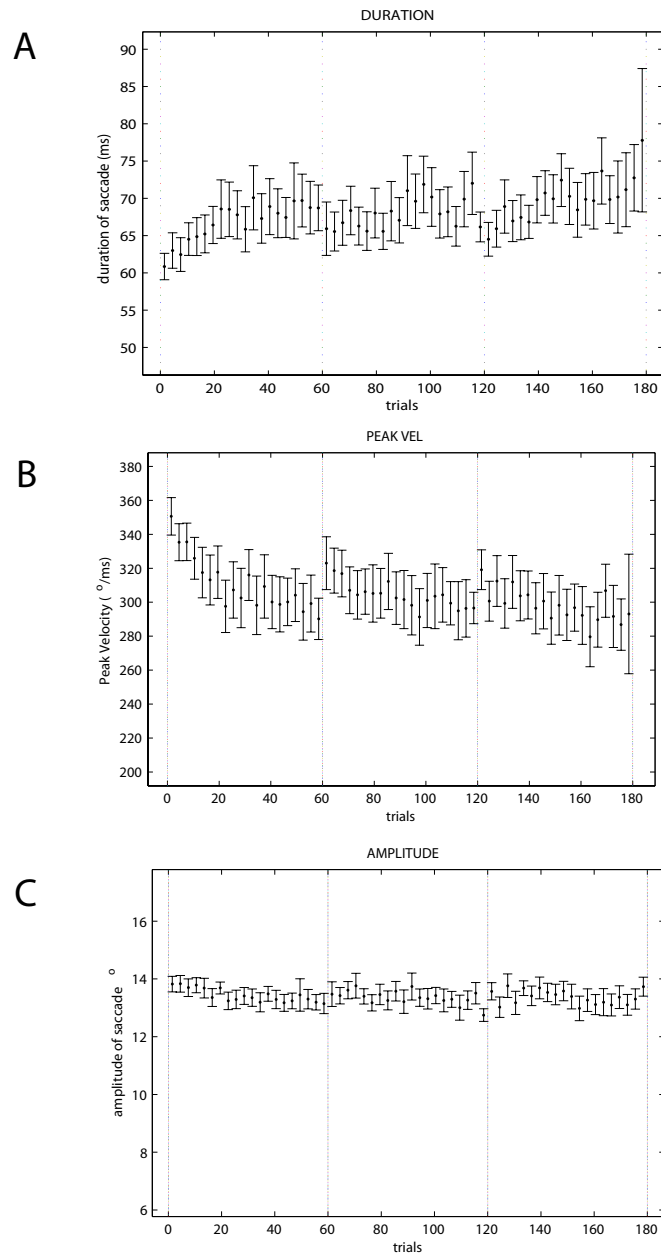


Figure 4.4: Sample of fatigue data. Three sets of 60 saccades repeatedly performed on a 15° target ($n=9$). **A.** Saccade duration increases across trials. **B.** Peak Velocity decreases across trials. **C.** Amplitude remains constant

Chapter 5

Gain-Adaptation Direction Engages

Different Adaptive Mechanisms

This chapter represents the latest part for this thesis. It is presented in a format similar to chapter 3, as it is the author's intent to submit it as an article in a scientific journal. The experimental evidence shown here demonstrates how the direction in which gain-adaptation occurs (gain-up or gain-down) determines the mechanism by which the saccadic apparatus is going to react to the disruption in target position. An optimal control model of saccade generation forms the basis to predict the important kinematic features of the data.

5.1 Materials and Methods

Subjects were recruited from our medical school community. The experiments were composed either of a standard double-step adaptation paradigm or of a mimic-adaptation paradigm, in which subjects made saccades to targets mimicking the end-point pattern of their performance in the double-step paradigm, but without inducing any adaptation. Group 1 subjects trained in a gain-down (decrease) paradigm and returned later for a paradigm in which the target positions were tailored to their own individual adaptation performance. Group 2 subjects trained in a gain-up (increase) paradigm and returned later for the mimic-adaptation paradigm. Five subjects participated in each group and acted as their own controls. There was at least a break of one day between the two experiments. Subjects gave written consent and the protocol was approved by the Johns Hopkins Institutional Review Board.

5.1.1 Experimental Setup

The position of either the right or the left eye was measured with a magnetic-field search-coil system [25] using directional scleral annuli (Skalar Medical BV, Delft, Netherlands). Raw coil signals were filtered in hardware (90-Hz low-pass Butterworth), digitized (1,000 Hz), and saved on computer for later analysis. Targets were rear-projected using a mirror-controlled laser beam of 2mm-diameter projected onto a translucent screen located 1m in front of the subject with a 15° step-response of faster than 10ms. The room was

CHAPTER 5. GAIN-ADAPTATION'S DIRECTION ENGAGE DIFFERENT ADAPTIVE MECHANISMS

otherwise dark. The head of the subjects was stabilized with a bite bar of dental impression material.

5.1.2 Experimental Paradigm

Saccade adaptation was induced using the standard double-step paradigm [26]. After the saccade adaptation experiment, the first saccade end-points of each subject were determined and used to form a sequence of targets to be shown to them during a later mimic-adaptation experiment. This paradigm consisted in a set of targets displayed in order to reproduce the subject's own end-point pattern of adaptation, only without eye-movement triggered target jumps and, therefore, without any stimulus for adaptation. Each experiment began with a sequence of error-clamp trials for baseline assessment (Ethier et al., 2008).

Group 1: Gain-down. Subjects performed 180 error-clamp trials consisting of 90, 60 and then 30 trials. They subsequently had 480 gain-down trials equally separated into eight sets of 60 trials. This data was then used to generate the targets for the later mimic-adaptation experiment. Compensating for the inherent hypometria of each individual, 480 (eight sets of 60 trials) more trials were introduced in a second experiment that aimed at closely reproducing the same first-saccade amplitudes as the ones measured in the first, adaptation experiment. This second experiment also began with 180 error-clamp trials like in the first one.

Group 2: Gain-up. For this group, subjects trained for gain-up, but otherwise experienced the same conditions as Group 1 in both experiments.

CHAPTER 5. GAIN-ADAPTATION'S DIRECTION ENGAGE DIFFERENT ADAPTIVE MECHANISMS

Adaptation trials. Trials began with a fixation target. At a random time in the range of 500-1000ms, the fixation target was turned off and target T1 appeared 15° away from it. Once the eye began moving toward T1, T1 was displaced to T2. The displacement was either 5° away from (gain-up) or 5° closer to (gain-down) the initial fixation point. The jump was triggered near the onset of the eye movement, defined as the moment where the eye crossed a virtual 2° window placed around the fixation point (only visible to the experimenter). Target T2 was maintained for 500ms, at which time the trial ended and T2 became the fixation point for the next trial in the opposite direction. Over time, subjects learned to make a saccade in response to T1 that was smaller (gain-down paradigm) or larger (gain-up paradigm). Each adaptation set consisted of 60 trials. The mean inter-trial time was 1250ms. Between sets, subjects received 30 seconds of rest, in which they were asked to close their eyes.

Mimic-adaptation trials. Trials began with a fixation target. At a random time in the range of 500-1000ms, the fixation target was turned off and target T1 was displayed at x_i° horizontal. T1 remained at x_i° for 700ms at which point the target moved to T2, which became the fixation point for the next trial (i+1) in the opposition direction. T2 was displayed at the same location as that of the corresponding adaptation trial. Each mimic-adaptation set consisted of 60 trials. The mean inter-trial time was 1450ms. The longer time spent at the final target (700ms in mimic-adaptation trials versus 500ms in adaptation trials) was set to allow subjects time to perform a second, corrective saccade to the target when necessary. Between sets, subjects received 30 seconds of rest, in which they were asked to close their

CHAPTER 5. GAIN-ADAPTATION'S DIRECTION ENGAGE DIFFERENT ADAPTIVE MECHANISMS

eyes.

Error-clamp trials. Trials began with a fixation target. At a random time in the range of 500-1000ms, the fixation target was turned off and target T1 was displayed at 15° horizontal. Once the saccade began, T1 disappeared and at 500 or 800ms later (Groups 1 and 2, respectively) the target reappeared at the position where the eye was located at 10ms prior (i.e., 490 or 790ms). In this way, first no and then a zero visual error was present after the saccade. Due to slight amplitude asymmetry between leftward and rightward saccade, occasionally a drift away from the center developed over time. We restrained eye position inside a +/-20-degree range by resetting the fixation point to +/-5 degrees whenever the eye landed out-of-bounds. The mean inter-trial time was 1250ms and 1550ms (for Groups 1 and 2, respectively).

5.1.3 Data Analysis

The duration of saccades was determined by a 20-deg/sec speed threshold. Discriminating criteria were used to dismiss abnormal saccades. Saccades were rejected (i) if they didn't reach a peak velocity higher than 90 deg/sec; (ii) if they had a latency less than 100ms; (iii) if they displayed multiple peaks in their speed profile; (iv) and finally if they were shorter than 50% of the target displacement. Most subjects had less than 5% of their saccade falling under one or more of these aforementioned criteria, with none of them exceeding 10% of all saccades.

5.2 Results

5.2.1 Saccade Kinematics

Fig.5.1A shows that, for Group 1, the first-saccade amplitude of the mimic-adaptation experiment is tightly tailored to the previous adaptation performance. The small, quick return to baseline in the amplitude plot (same figure) due to the forgetting occurring during the 30-second breaks has also been mimicked in the control condition. Although the amplitudes seem to be virtually the same throughout the whole experiment, Fig.5.1B-F demonstrate that the trajectories employed to reach the same eccentricities are radically different between the two conditions. In general, a gain-down adapted saccade is slower and longer compared to its 'normal' counterpart; or, in terms of the kinematics of the saccade, a smaller initial acceleration phase along with a lighter deceleration toward the end of the movement entails a smaller, later peak velocity and a longer duration for the adaptation condition.

The features measured in Group 1 are in great contrast with that of Group 2. Fig.5.2 includes the corresponding plots for gain-up adaptation. We observed that, in this case, the adaptation kinematics are indistinguishable from that of the mimic-adaptation condition. As far as the trajectory characteristics are concerned, contrary to inducing a reduction in saccade amplitude, extending the length of a saccade through gain-adaptation seems to be equivalent to gradually (trial after trial) displacing a target away from its initial location.

We performed a statistical analysis of the data to determine if the changes seen be-

CHAPTER 5. GAIN-ADAPTATION'S DIRECTION ENGAGE DIFFERENT ADAPTIVE MECHANISMS

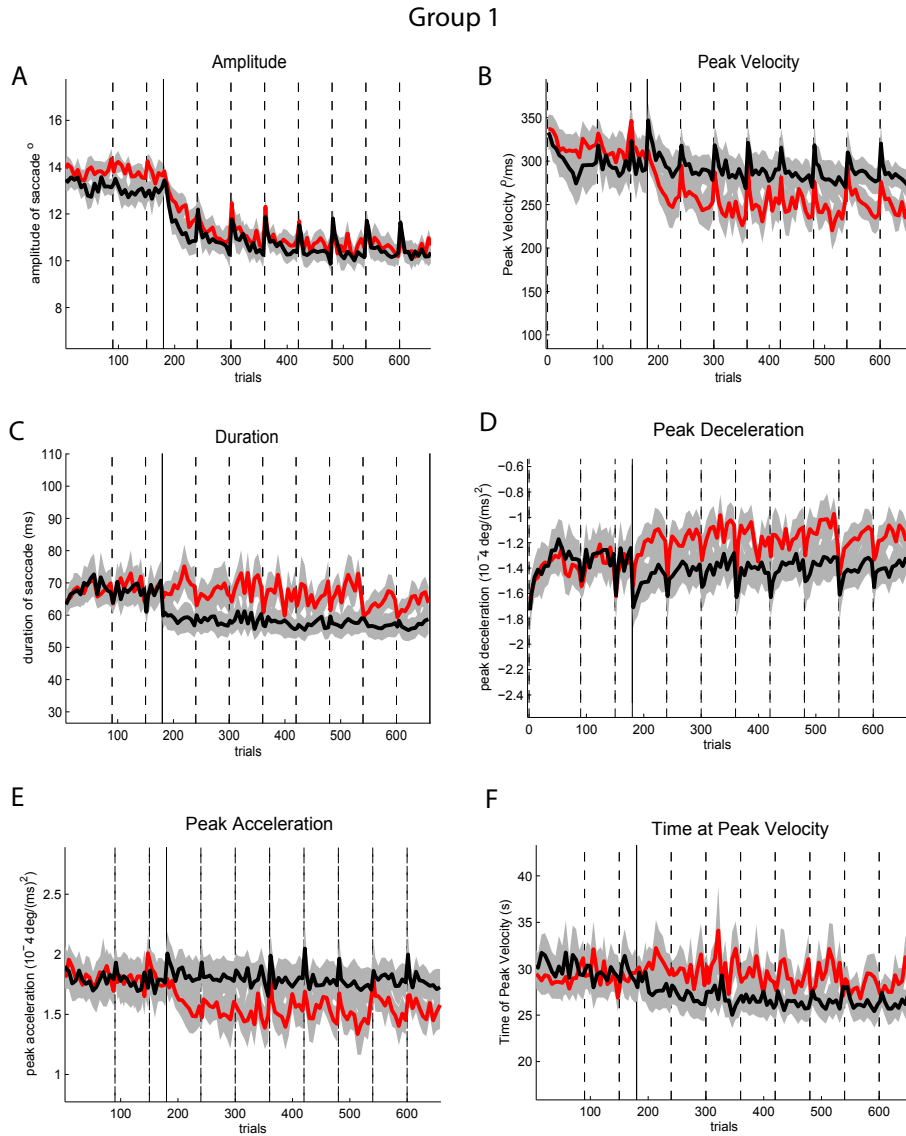


Figure 5.1: Trial-by-trial saccade characteristics for gain-down adaptation versus corresponding mimic-adaptation. The dotted lines represent set breaks and the solid line divides the error-clamp trials from the adaptation/mimic-adaptation trials. In red are the mean adaptation kinematics and in black the mean mimic-adaptation's ($n=5$). **A.** Amplitude in degrees. **B.** Peak velocity in degrees per second. **C.** Saccade duration in milliseconds. **D.** Peak Deceleration in degrees per second squared. **E.** Peak Acceleration in degrees per second squared. **F.** Time with respect to saccade onset at which the velocity reaches its peak. In each set, the bin size was two trials for the first bin, then four trials, then six trials for all subsequent bins for that set.

CHAPTER 5. GAIN-ADAPTATION'S DIRECTION ENGAGE DIFFERENT ADAPTIVE MECHANISMS

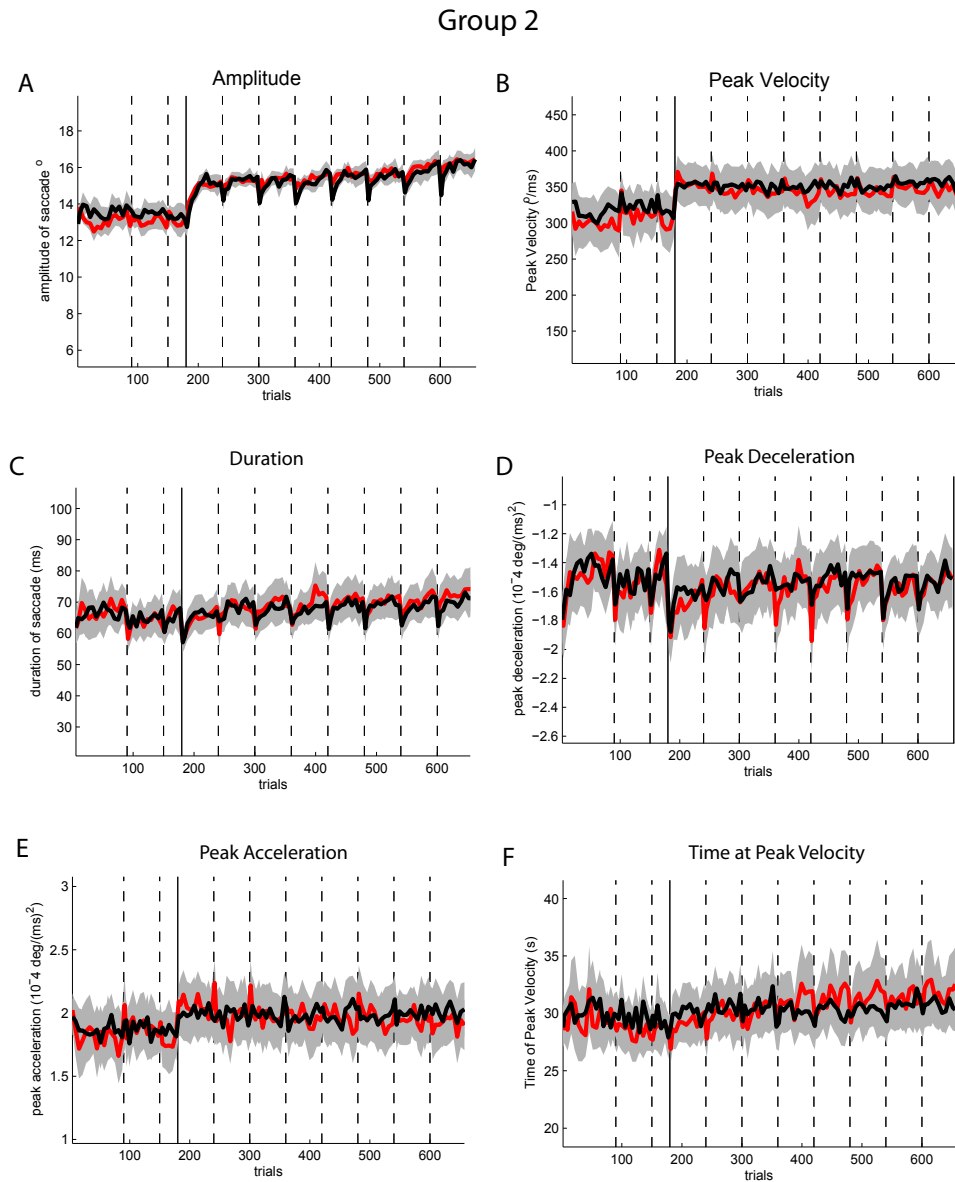


Figure 5.2: Trial-by-trial saccade characteristics for gain-up adaptation versus corresponding mimic-adaptation. The dotted lines represent set breaks and the solid line divides the error-clamp trials from the adaptation/mimic-adaptation trials. In red are the mean adaptation kinematics and in black the mean mimic-adaptation's ($n=5$). **A.** Amplitude in degrees. **B.** Peak velocity in degrees per second. **C.** Saccade duration in milliseconds. **D.** Peak Deceleration in degrees per second squared. **E.** Peak Acceleration in degrees per second squared. **F.** Time with respect to saccade onset at which the velocity reaches its peak. In each set, the bin size was two trials for the first bin, then four trials, then six trials for all subsequent bins for that set.

CHAPTER 5. GAIN-ADAPTATION'S DIRECTION ENGAGE DIFFERENT ADAPTIVE MECHANISMS

tween the two conditions were significant. To do so, we used repeated-measures one-way ANOVA tests on the mean of each of the kinematics presented in Fig.5.1 and 5.2. These means were computed from the last 40 trials of the last 7 sets of the adaptation phase. The entire first set and the first 20 trials of each subsequent sets were left out because we wished to test the stationary phase of the data, avoiding variability stemming from transient states. Fig.5.3 shows a summary of the results of the analysis. For Group 1, the amplitude was reduced to an average of 10.41° in the mimic-adaptation condition and to 10.66° in the adaptation condition; the difference was insignificant. However, the mean peak velocity significantly differed between the two conditions ($281.4^\circ/sec$ and $241.80^\circ/sec$, respectively. $F(4,1) = 8.87, p < 0.05$) and so did the mean duration ($56.7ms$ and $68.7ms$, respectively. $F(4,1) = 13.54, p < 0.05$). As could be expected, the peak acceleration was significantly smaller ($18.6kdeg/sec^2$ versus $14.8kdeg/sec^2$. $F(4,1) = 9.04, p < 0.05$) and the peak deceleration significantly smaller too ($-14.7kdeg/sec^2$ versus $-10.8kdeg/sec^2$. $F(4,1) = 7.95, p < 0.05$) in the adaptation condition. In contrast, there was no statistical difference across conditions for any of the kinematics computed in Group 2. It appears that saccades made through gain-up adaptation are indistinguishable from the ones made to normal, non-jumping target.

5.2.2 Saccade Latencies

In attempting to characterize the differences between a 'normal' and an 'adapted' saccade, we also looked into saccade latencies as a possible discriminating measure. Saccade

CHAPTER 5. GAIN-ADAPTATION'S DIRECTION ENGAGE DIFFERENT ADAPTIVE MECHANISMS

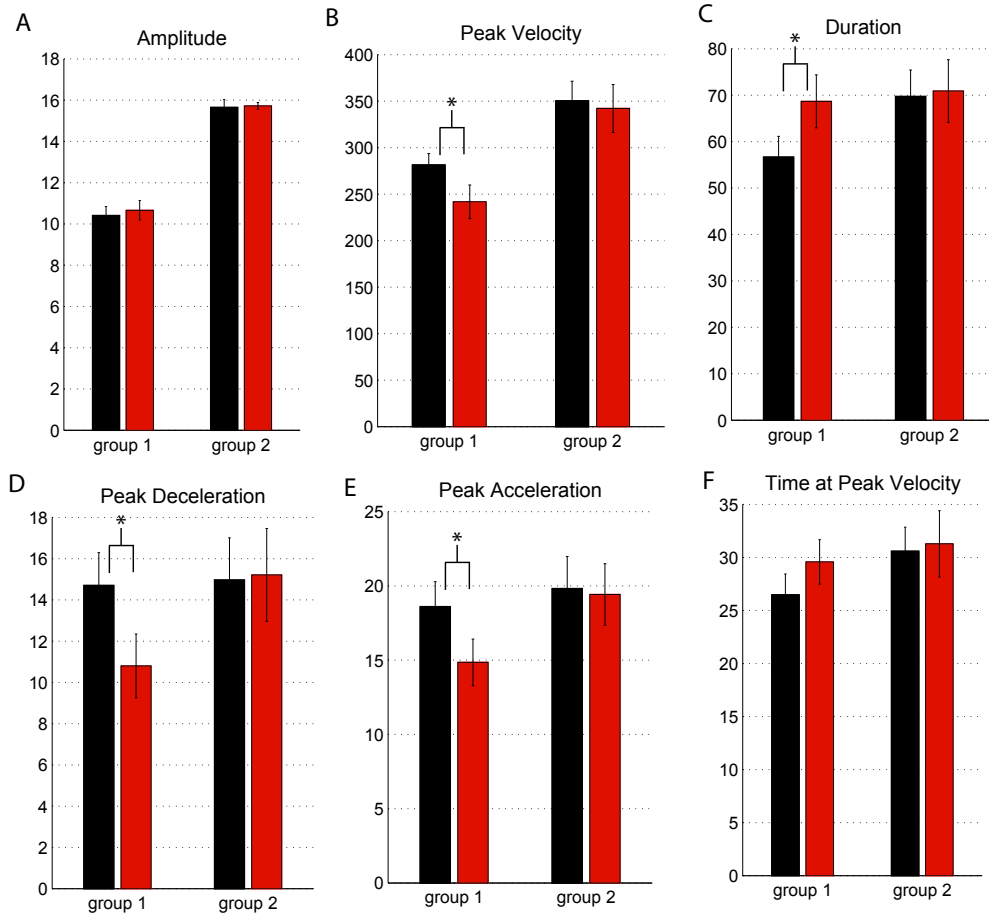


Figure 5.3: Bar plots for adaptation vs mimic-adaptation comparison. Red is adaptation condition and black is control condition. Error bars are SEM. **A.** There was no statistical difference between the two conditions for each group **B.** The peak velocity significantly differed in Group 1. The peak velocity was smaller for the adaptation condition. **C.** Saccade duration was significantly larger for the adaptation condition in Group 1. There was no difference in Group 2 **D & E.** Peak deceleration and peak acceleration were both significantly smaller for the mimic-adaptation condition in Group 1. No significant difference was found in Group 2. **F.** In each group, no significant difference could be concluded for the time at peak velocity kinematics. Nonetheless, the difference was close to significant in Group 1 (shorter time at peak velocity for the mimic-adaptation condition, $F(4, 1) = 5.27$, $p = 0.083$)

CHAPTER 5. GAIN-ADAPTATION'S DIRECTION ENGAGE DIFFERENT ADAPTIVE MECHANISMS

latency is defined as the time it took for the eye to initiate a saccade with respect to the time at which the target was displayed. As can be seen in Fig.5.4A, there is a striking difference between the two conditions in Group 1. Calculating and comparing mean latencies in the same fashion as we did for the other kinematics, we concluded that adapted saccades take much longer to begin than normal ones for that group (161.3ms versus 214.3ms. $F(4, 1) = 84.77, p < 0.001$). In Group 2, Fig.5.4B shows that the difference is less, but still significant; adapted saccades have longer latencies in a gain-up paradigm as well (185.27ms versus 202.32ms. $F(4, 1) = 13.23, p < 0.05$).

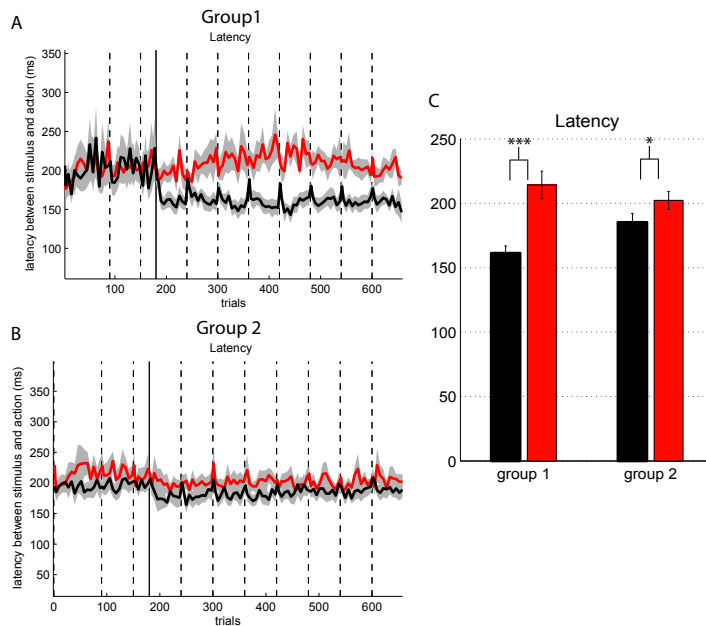


Figure 5.4: Saccade latency trial-by-trial and bar plot. Red is adaptation condition and black is control condition. **A & B.** Saccade latency in milliseconds for Group 1 and 2. Dotted lines represent set breaks and solid line marks the end of error-clamp trials **C.** Bar plot for mean values. Error bars are SEM.

5.3 Discussion

5.3.1 Forward model adaptation versus adaptation via target remapping

Referring to the saccade modeling presented in chapter 4, we propose a novel interpretation for the critical changes in kinematics that we observed when subjects made eye movements to a target that repeatedly jumped either shorter than or farther from its initial location. The optimal control problem for a saccadic movement has been formulated as follows: at each time step t , find the motor command \mathbf{u}_t that minimizes the cost-to-go

$$J = \sum_t \mathbf{x}_t^T Q_t \mathbf{x}_t + \mathbf{u}_t^T R \mathbf{u}_t \quad (5.1)$$

under the constraints of the dynamics of the system:

$$\mathbf{x}_{t+1} = A\mathbf{x}_t + B\mathbf{u}_t \quad ; \quad \mathbf{x} := [x, \dot{x}, r]^T \quad (5.2)$$

The solution to this problem is

$$\mathbf{u}_t = -G_t \hat{\mathbf{x}}_t \quad (5.3)$$

Notice that, unlike Eq.4.8, Eq.5.3 uses an estimate $\hat{\mathbf{x}}_t$ of the state vector in the control policy. The reason for this is that the learner may not have access to the true position and velocity of the eye ball at each time step and consequently has to form an estimate of it. Because a typical saccade happens so fast (usually in the 40 – 80ms range), there is no time for sensory information (e.g. proprioception, vision) to contribute to this estimate.

CHAPTER 5. GAIN-ADAPTATION'S DIRECTION ENGAGE DIFFERENT ADAPTIVE MECHANISMS

The nervous system has to rely instead on a so-called forward model that determines the estimate in-flight and then use it to send the appropriate motor commands dynamically. Using an efferent copy of the motor commands \mathbf{u}_t that were just sent and the last estimate $\hat{\mathbf{x}}_t$, the learner can estimate \mathbf{x}_{t+1} through an internal model of the eye plant:

$$\hat{\mathbf{x}}_{t+1} = \hat{A}\hat{\mathbf{x}}_t + \hat{B}\mathbf{u}_t \quad (5.4)$$

where \hat{A} and \hat{B} are the learner's estimates of the matrices reflecting the physics of the motor plant.

After honing it through gazillions of saccades, it is reasonable to assume that the forward model is well calibrated and highly accurate, and so $\hat{A} = A$ and $\hat{B} = B$.

However, when a sudden error is introduced through an intrasaccadic target step, the learner can assign this error to a failure in the forward model and therefore make temporary adjustments to it. Additionally, the error can be assigned to an inadequate choice of target goal r and modify it accordingly for the next trials. We believe this credit assignment problem is at the core of the way a saccade adapts to minimize the error. Because saccades adapt so differently to a consistent target jump depending if it is in one direction or in the opposite, we posit that a strong shift occurs in the way the brain assigns the error when it switches direction. Fig.5.5 describes in terms of the parameters of the model how the nervous system might be dealing with this vectorized error. The learner can respond to the error by either remapping the target, in which case $r' = r + \Delta r$, or by resorting to make adjustments in the forward model. This last alternative is modeled here as a change in the effect of the efferent copy of the motor commands on the estimate $\hat{\mathbf{x}}$ of the state vector. The

CHAPTER 5. GAIN-ADAPTATION'S DIRECTION ENGAGE DIFFERENT ADAPTIVE MECHANISMS

learner can thus modulate its belief about the effects of the motor commands it is sending on the state of the eye. If, for example, the learner faces a consistent overshoot of the target, it might start to believe that the motor commands it sends have a stronger effect on the dynamics of the eye than it had initially expected. In concrete terms, \hat{B} is in fact equal to $(1 - \beta)B$ and is thus parametrized by a factor β to either diminish or increase the impact of \mathbf{u}_t in Eq.5.4. Fig.5.6 shows a simulation of this model that illustrates an amplitude-decreased saccade through each of the two proposed mechanisms. This cartoon reproduces nicely the features of Group 1 shown in Fig.5.1.

Why would gain-up and gain-down be mediated by so inherently different mechanisms? First, it is clear that amplitude increases only fully adapt to target jumps that are much smaller in comparison to amplitude decreases [45–47]. This asymmetry can be explained by a simple system of two mechanisms of adaptation and is arguably more likely than a single mechanism with direction-dependent effects on kinematics as well as different saturation levels. Second, typical saccades usually undershoot the target, a phenomenon called hypometria. Given a retinal target location, a mechanism must be already in place to induce the impending saccade into this hypometric state; we here suggest this mechanism to be mainly forward-model-dependent. Overshoot, on the contrary, seldom happens and might consequently arouse an alternate system to compensate for the error, possibly a retinal remapping of the target. In addition, to prevent avoid any loss of generality, we propose that a mixture of the two mechanisms of adaptation are engaged when unexpected error arises, not that each of them is used exclusively for errors in one direction. The asymmetry

CHAPTER 5. GAIN-ADAPTATION'S DIRECTION ENGAGE DIFFERENT ADAPTIVE MECHANISMS

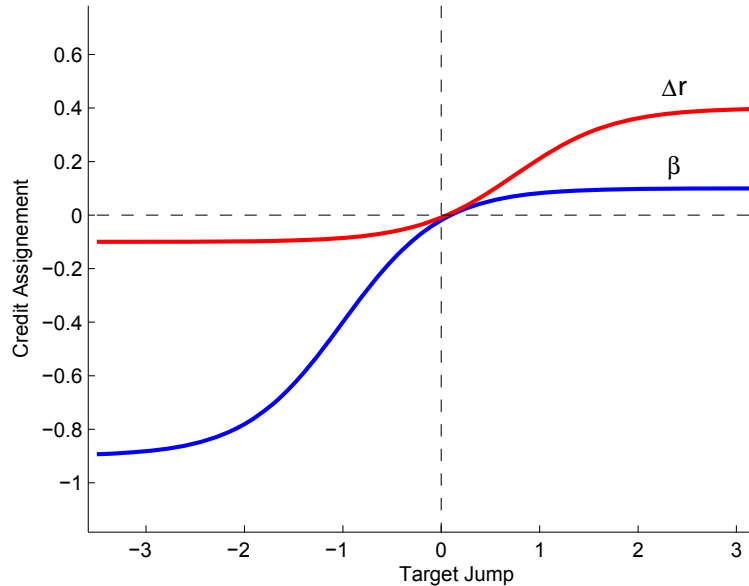


Figure 5.5: Credit assignment as a function of target-jump size and direction. Positive error indicates a displacement of the target away from its initial position (Gain-Up). Negative error indicates a displacement of the target toward the initial fixation point (Gain-Up). The learner can respond to the error induced by a jumping target by remapping the target and by updating its forward model through parameter β (red and blue curve, respectively). Note the dissymmetry in total adaptation between the two directions accounting for the inability to adapt to a forward target jump as much as for a backward jump. In each direction, however, both mechanisms of adaptation saturate as the jump size increases. The saturation level is normalized for the backward jump direction. At each point on the x-axis, the relative contribution of each mechanism can be estimated by dividing one curve by the sum of the two.

in the data arises because each mechanism is more predominantly used in one direction than in the other. This idea relates to earlier work from [48] on adaptation fields, which argued that gain-up instigated mainly a remapping of the target, whereas gain-down employed a separate mechanism responsible for gain reduction.

An apparent limit of this model is that it gives no insights about the trial-by-trial, error-dependent evolution of adaptation in time. However, we can show that it could be upgraded

CHAPTER 5. GAIN-ADAPTATION'S DIRECTION ENGAGE DIFFERENT ADAPTIVE MECHANISMS

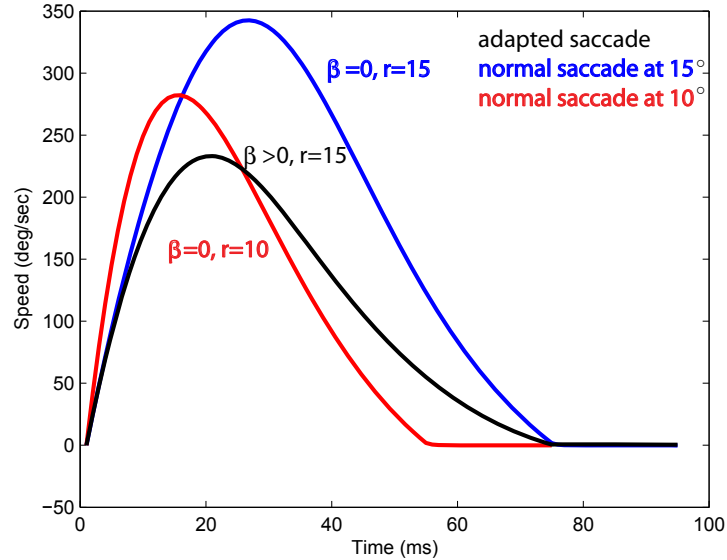


Figure 5.6: Saccade simulation for Gain-Down adaptation. In blue, an unadapted saccade profile directed to a 15-degree target. In red, a completely remapped saccade profile of 10-degree amplitude. In black, a full forward model adaptation to 10 degrees from a 15-degree initial target eccentricity.

to account for this without much difficulty. For example, one could imagine a scenario where a *fraction* of the perceived error would contribute to 'push' the state of the learner on the curves in Fig.5.5 to reach a further adapted state. To make matters more complex, the adapted state could have its own time scales: one could add a trial-dependent forgetting rate dragging the state toward the center. These add-ons to the model presented above are, of course, relevant, but we argue that they would not do much help to explain the basic kinematics changes in the data.

As they are surveyed in chapter 2, the SC and the cerebellum are most probably the major components of the saccade circuitry undergoing the important changes in activity

CHAPTER 5. GAIN-ADAPTATION'S DIRECTION ENGAGE DIFFERENT ADAPTIVE MECHANISMS

triggering saccade adaptation. Since during adaptation the SC, the pathway to the cerebellum (NRTP), and the cerebellum have been shown to modify their pattern of activation [13, 18, 49], it is hard to pinpoint a single locus where the proposed mechanisms of adaptation would occur. However, if the neural substrates of the two mechanisms of adaptation are physically separate at least at one location in the saccadic circuitry, it should necessarily be possible to shut down one of them and inactivate adaptation in one direction, but not in the other.

5.3.2 Why latencies vary between groups and between conditions

Latencies are significantly different across conditions and across groups. Group 1 in the mimic-adaptation condition has the lowest latency ($161.3 \pm 5.6ms$). Then, comes Group 2 in the mimic-adaptation condition ($185.3 \pm 6.9ms$). Third and Fourth comes Group 2 and Group 1 in the adaptation condition ($202.3 \pm 6.9ms$ and $214.3 \pm 10.7ms$).

We identified three possible causes for the difference in latencies that were observed. First, control data (not shown here) suggests that latency depends, to some extent, on target eccentricity. Generally, the farther the target, the longer it takes to initiate a saccade. Second, saccade latency could be context-dependent. One can think of the decision to make a saccade as a trade-off between the cost of not foveating the target (lack of information due to low resolution in the peripheral vision) and the cost of initiating the saccade (risk of

CHAPTER 5. GAIN-ADAPTATION'S DIRECTION ENGAGE DIFFERENT ADAPTIVE MECHANISMS

losing track of the target if it suddenly moves while the saccade is underway, for example). This line of thinking is defended in [50] and then later in [51] where they found that the latency required to make a saccade to a shifting target consisting of two concentric rings is larger when attending to the larger of the two rings (lower cost of not making a saccade). In the error-clamp trials, the target disappears altogether as soon as the eye moves, so it makes sense that the latency in error-clamp trials is larger than that for saccades directed toward fixed targets. This rationale also predicts that an adaptation trial should be of higher latency than for a mimic-adaptation trial, because of the cost-rising intrasaccadic jump of the former. Third, if indeed two different mechanisms of adaptation are at play during gain-adaptation, chances are that the latency associated with each of them is different.

In that light, we can make sense of the latency data as follows. Let us assume for simplification purposes that gain-down is purely a forward model adaptation and that gain-up is a pure remapping process. Rounding the numbers in the two mimic-adaptation conditions, there is approximately a 25 ms eccentricity-dependent latency difference between gazing at a 10-degree target and a 16-degree target. Considering now Group 2, the only explanation for a difference in latency would be the context-dependent effect (same eccentricity, no forward model adaptation). Therefore, still keeping the numbers round, making saccades to targets that jump extends latency by around 15 ms. Finally, the latency data in Group 1 can be explained by two factors. Subtracting the context-dependent effect, we find that forward model adaptation requires an extra 40 ms compared to what it would take to remap the target. We conclude that this number must reflect the additional processing time

required when mainly relying on forward model adaptation.

5.3.3 Other related gain-adaptation saccade studies

Additional research studies previously examined changes in kinematics evoked by gain-adaptation. However, these studies have yielded rather conflicting results. The most relevant to this study, [52] recently found that gain-down adaptation in humans caused saccades to last longer and was characterized by a smaller peak deceleration; this is consistent with our data. They however determined that all other kinematics remained unchanged when compared to control saccades of the same amplitude. First of all, a change in duration has to imply a counterbalancing change in another kinematics for saccades to keep the same amplitude. If the peak velocity is not smaller, another measure necessarily changed somewhere or else some important experimental flaws would completely discredit their report. Moreover, their methodology was substantially different than the one we used. They adapted saccades with smaller amplitude and a total gain-change of less than 20% (Group 1 \approx 30%), which may have prevented detection of significant dynamic transformations. Fixation points were randomly assigned between different locations, whereas we kept them constant. Finally, control data was recorded by randomly sweeping across targets of different amplitude in the same experiment before the adaptation phase, in contrast with our mimic-adaptation paradigm. Similar in methodology was reminiscent of [53] who examined both gain-up and gain-down adaptation. Their conclusions were that for amplitude increases, duration was longer and peak velocity, shorter than their controls. This opposes

CHAPTER 5. GAIN-ADAPTATION'S DIRECTION ENGAGE DIFFERENT ADAPTIVE MECHANISMS

our results that the two conditions in Group 2 are kinematically indistinguishable. As for amplitude decreases, no significant change could be detected as far as duration and peak velocity are concerned. The average level of adaptation in gain-down was considerably smaller than ours (20%), even though the step jump was set to 30%. This is probably due to the fact that several amplitudes were adapted in parallel. This detail may be an important confounding factor as the existence of adaptation fields [47] - the effect of generalizing adaptation onto other target eccentricity - may be a factor interfering with the overall adaptation process, in an unpredictable manner. In rhesus monkeys, [54] reported an increase in peak velocity accompanying gain-down adaptation, which is opposite to our findings, whereas [17] rather saw a drop in peak velocity as we did.

None of these studies have used the same methodology to assess the effects of adaptation. The mimic-adaptation condition used here for the first time is a particularly efficient way to compare one's adaptation performance against its own control saccades across a large number of trials because it limits the amount of confounding factors to a minimum. We think that this paradigm, had it been used in these other studies, would have done great help to reconcile their results with ours - as well as with each other's.

5.4 Conclusion

We put forward here important, yet until now unknown, differences that exist between training a subject in a gain-down versus gain-up paradigm. These differences led to the

CHAPTER 5. GAIN-ADAPTATION'S DIRECTION ENGAGE DIFFERENT ADAPTIVE MECHANISMS

hypothesis of two, rather than one, distinct mechanisms responsible for saccade adaptation (forward model adaptation versus target remapping). As more knowledge is gained from neurophysiological studies, we believe evidence about the loci and neural-level functioning of these two mechanisms will be brought to light.

Bibliography

- [1] C. Scudder, C. Kaneko, and A. Fuchs, “The brainstem burst generator for saccadic eye movements: a modern synthesis,” *Exp Brain Res*, vol. 142, pp. 439–462, Feb 2002.
- [2] J. Harting, “Descending pathways from the superior colliculus: an autoradiographic analysis in the rhesus monkey (*Macaca mulatta*),” *J. Comp. Neurol.*, vol. 173, pp. 583–612, Jun 1977.
- [3] K. Kawamura, A. Brodal, and G. Hoddevik, “The projection of the superior colliculus onto the reticular formation of the brain stem. An experimental anatomical study in the cat,” *Exp Brain Res*, vol. 19, pp. 1–19, Jan 1974.
- [4] A. Fuchs, C. Kaneko, and C. Scudder, “Brainstem control of saccadic eye movements,” *Annu. Rev. Neurosci.*, vol. 8, pp. 307–337, 1985.
- [5] C. Scudder, “A new local feedback model of the saccadic burst generator,” *J. Neurophysiol.*, vol. 59, pp. 1455–1475, May 1988.

BIBLIOGRAPHY

- [6] J. Van Gisbergen, D. Robinson, and S. Gielen, "A quantitative analysis of generation of saccadic eye movements by burst neurons," *J. Neurophysiol.*, vol. 45, pp. 417–442, Mar 1981.
- [7] J. Hopp and A. Fuchs, "The characteristics and neuronal substrate of saccadic eye movement plasticity," *Prog. Neurobiol.*, vol. 72, pp. 27–53, Jan 2004.
- [8] R. Batton, A. Jayaraman, D. Ruggiero, and M. Carpenter, "Fastigial efferent projections in the monkey: an autoradiographic study," *J. Comp. Neurol.*, vol. 174, pp. 281–305, Jul 1977.
- [9] D. Zee, R. Yee, D. Cogan, D. Robinson, and W. Engel, "Ocular motor abnormalities in hereditary cerebellar ataxia," *Brain*, vol. 99, pp. 207–234, Jun 1976.
- [10] Y. Iwamoto and K. Yoshida, "Saccadic dysmetria following inactivation of the primate fastigial oculomotor region," *Neurosci. Lett.*, vol. 325, pp. 211–215, Jun 2002.
- [11] L. Ritchie, "Effects of cerebellar lesions on saccadic eye movements," *J. Neurophysiol.*, vol. 39, pp. 1246–1256, Nov 1976.
- [12] L. Optican and F. Miles, "Visually induced adaptive changes in primate saccadic oculomotor control signals," *J. Neurophysiol.*, vol. 54, pp. 940–958, Oct 1985.
- [13] C. Scudder and D. McGee, "Adaptive modification of saccade size produces correlated changes in the discharges of fastigial nucleus neurons," *J. Neurophysiol.*, vol. 90, pp. 1011–1026, Aug 2003.

BIBLIOGRAPHY

- [14] Y. Kojima, Y. Iwamoto, F. Robinson, C. Noto, and K. Yoshida, "Premotor inhibitory neurons carry signals related to saccade adaptation in the monkey," *J. Neurophysiol.*, vol. 99, pp. 220–230, Jan 2008.
- [15] D. Sparks, R. Holland, and B. Guthrie, "Size and distribution of movement fields in the monkey superior colliculus," *Brain Res.*, vol. 113, pp. 21–34, Aug 1976.
- [16] J. Wallman and A. Fuchs, "Saccadic gain modification: visual error drives motor adaptation," *J. Neurophysiol.*, vol. 80, pp. 2405–2416, Nov 1998.
- [17] M. Frens and A. Van Opstal, "Monkey superior colliculus activity during short-term saccadic adaptation," *Brain Res. Bull.*, vol. 43, pp. 473–483, 1997.
- [18] N. Takeichi, C. Kaneko, and A. Fuchs, "Activity changes in monkey superior colliculus during saccade adaptation," *J. Neurophysiol.*, vol. 97, pp. 4096–4107, Jun 2007.
- [19] B. Melis and J. van Gisbergen, "Short-term adaptation of electrically induced saccades in monkey superior colliculus," *J. Neurophysiol.*, vol. 76, pp. 1744–1758, Sep 1996.
- [20] J. Edelman and M. Goldberg, "Effect of short-term saccadic adaptation on saccades evoked by electrical stimulation in the primate superior colliculus," *J. Neurophysiol.*, vol. 87, pp. 1915–1923, Apr 2002.
- [21] K. Myers and M. Davis, "Behavioral and neural analysis of extinction," *Neuron*, vol. 36, pp. 567–584, Nov 2002.

BIBLIOGRAPHY

- [22] Y. Kojima, Y. Iwamoto, and K. Yoshida, “Memory of learning facilitates saccadic adaptation in the monkey,” *J. Neurosci.*, vol. 24, pp. 7531–7539, Aug 2004.
- [23] M. Smith, A. Ghazizadeh, and R. Shadmehr, “Interacting adaptive processes with different timescales underlie short-term motor learning,” *PLoS Biol.*, vol. 4, p. e179, Jun 2006.
- [24] R. Scheidt, D. Reinkensmeyer, M. Conditt, W. Rymer, and F. Mussa-Ivaldi, “Persistence of motor adaptation during constrained, multi-joint, arm movements,” *J. Neurophysiol.*, vol. 84, pp. 853–862, Aug 2000.
- [25] D. Robinson, “A method of measuring eye movement using a scleral search coil in a magnetic field,” *IEEE Trans Biomed Eng.*, vol. 10, pp. 137–145, Oct 1963.
- [26] S. McLaughlin, “Parametric adjustment in saccadic eye movements,” *Percept Psychophys.*, vol. 2, pp. 359–362, Oct 1967.
- [27] P. van Overschee and B. De Moor, *Subspace identification for linear systems*, K. Academic, Ed. Springer, 1996.
- [28] H. Collewijn, C. Erkelens, and R. Steinman, “Binocular co-ordination of human horizontal saccadic eye movements,” *J. Physiol. (Lond.)*, vol. 404, pp. 157–182, Oct 1988.
- [29] F. Bonnetblanc and P. Baraduc, “Saccadic adaptation without retinal postsaccadic error,” *Neuroreport*, vol. 18, pp. 1399–1402, Aug 2007.

BIBLIOGRAPHY

- [30] K. Kording, J. Tenenbaum, and R. Shadmehr, “The dynamics of memory as a consequence of optimal adaptation to a changing body,” *Nat. Neurosci.*, vol. 10, pp. 779–786, Jun 2007.
- [31] T. Seeberger, C. Noto, and F. Robinson, “Non-visual information does not drive saccade gain adaptation in monkeys,” *Brain Res.*, vol. 956, pp. 374–379, Nov 2002.
- [32] C. Noto and F. Robinson, “Visual error is the stimulus for saccade gain adaptation,” *Brain Res Cogn Brain Res*, vol. 12, pp. 301–305, Oct 2001.
- [33] J. Shafer, C. Noto, and A. Fuchs, “Temporal characteristics of error signals driving saccadic gain adaptation in the macaque monkey,” *J. Neurophysiol.*, vol. 84, pp. 88–95, Jul 2000.
- [34] M. Takagi, D. Zee, and R. Tamargo, “Effects of lesions of the oculomotor vermis on eye movements in primate: saccades,” *J. Neurophysiol.*, vol. 80, pp. 1911–1931, Oct 1998.
- [35] S. Barash, A. Melikyan, A. Sivakov, M. Zhang, M. Glickstein, and P. Thier, “Saccadic dysmetria and adaptation after lesions of the cerebellar cortex,” *J. Neurosci.*, vol. 19, pp. 10 931–10 939, Dec 1999.
- [36] F. Robinson, A. Fuchs, and C. Noto, “Cerebellar influences on saccade plasticity,” *Ann. N. Y. Acad. Sci.*, vol. 956, pp. 155–163, Apr 2002.
- [37] V. Bracha, L. Zhao, K. Irwin, and J. Bloedel, “The human cerebellum and associative

BIBLIOGRAPHY

- learning: dissociation between the acquisition, retention and extinction of conditioned eyeblinks,” *Brain Res.*, vol. 860, pp. 87–94, Mar 2000.
- [38] J. Medina, K. Garcia, and M. Mauk, “A mechanism for savings in the cerebellum,” *J. Neurosci.*, vol. 21, pp. 4081–4089, Jun 2001.
- [39] F. Shutoh, M. Ohki, H. Kitazawa, S. Itohara, and S. Nagao, “Memory trace of motor learning shifts transsynaptically from cerebellar cortex to nuclei for consolidation,” *Neuroscience*, vol. 139, pp. 767–777, May 2006.
- [40] H. Chen-Harris, W. Joiner, V. Ethier, D. Zee, and R. Shadmehr, “Adaptive control of saccades via internal feedback,” *J. Neurosci.*, vol. 28, pp. 2804–2813, Mar 2008.
- [41] D. Jirenhed, F. Bengtsson, and G. Hesslow, “Acquisition, extinction, and reacquisition of a cerebellar cortical memory trace,” *J. Neurosci.*, vol. 27, pp. 2493–2502, Mar 2007.
- [42] E. Todorov, “Stochastic optimal control and estimation methods adapted to the noise characteristics of the sensorimotor system,” *Neural Comput*, vol. 17, pp. 1084–1108, May 2005.
- [43] D. Robinson, “The systems approach to the oculomotor system,” *Vision Res.*, vol. 26, pp. 91–99, 1986.
- [44] E. Keller, “Accommodative vergence in the alert monkey. Motor unit analysis,” *Vision Res.*, vol. 13, pp. 1565–1575, Aug 1973.

BIBLIOGRAPHY

- [45] J. Miller, T. Anstis, and W. Templeton, "Saccadic plasticity: parametric adaptive control by retinal feedback," *J Exp Psychol Hum Percept Perform*, vol. 7, pp. 356–366, Apr 1981.
- [46] A. Straube, A. Fuchs, S. Usher, and F. Robinson, "Characteristics of saccadic gain adaptation in rhesus macaques," *J. Neurophysiol.*, vol. 77, pp. 874–895, Feb 1997.
- [47] C. Noto, S. Watanabe, and A. Fuchs, "Characteristics of adaptation fields produced by behavioral changes in saccade size and direction," *J. Neurophysiol.*, vol. 81, pp. 2798–2813, Jun 1999.
- [48] J. Semmlow, G. Gauthier, and J. Vercher, "Mechanisms of short-term saccadic adaptation," *J Exp Psychol Hum Percept Perform*, vol. 15, pp. 249–258, May 1989.
- [49] N. Takeichi, C. Kaneko, and A. Fuchs, "Discharge of monkey nucleus reticularis tegmenti pontis neurons changes during saccade adaptation," *J. Neurophysiol.*, vol. 94, pp. 1938–1951, Sep 2005.
- [50] L. Madelain, R. Krauzlis, and J. Wallman, "Spatial deployment of attention influences both saccadic and pursuit tracking," *Vision Res.*, vol. 45, pp. 2685–2703, Sep 2005.
- [51] M. Harwood, L. Madelain, R. Krauzlis, and J. Wallman, "The spatial scale of attention strongly modulates saccade latencies," *J. Neurophysiol.*, vol. 99, pp. 1743–1757, Apr 2008.

BIBLIOGRAPHY

- [52] T. Collins, A. Semroud, E. Orriols, and K. Dor-Mazars, “Saccade dynamics before, during, and after saccadic adaptation in humans,” *Invest. Ophthalmol. Vis. Sci.*, vol. 49, pp. 604–612, Feb 2008.
- [53] A. Straube and H. Deubel, “Rapid gain adaptation affects the dynamics of saccadic eye movements in humans,” *Vision Res.*, vol. 35, pp. 3451–3458, Dec 1995.
- [54] E. Fitzgibbon, M. Goldberg, and M. Segraves, “Short term adaptation in the monkey,” in *Adaptive Processes in Visual and Oculomotor Systems (Keller,EL.,Zee,DS.)*. Oxford: Pergamon Press, pp. 329–333, 1986.

Vita

Vincent Ethier was born and raised by his proud mother in the French-speaking half of Montreal: St-Leonard and then Anjou beach. In 2006, Vincent Ethier received a B.S. in Engineering Physics from Ecole Polytechnique Montreal, Canada, as well as a combined B.S. and M.Sc. in Engineering from Ecole Polytechnique, France; this accelerated education was made possible through a special partnership between the two universities. He subsequently enrolled and graduated from the Masters in Biomedical Engineering program of Johns Hopkins University in the spring of 2008. Upon graduation, Vincent will be exploring the mysterious lands of the Manchuria region or at least might be able to observe them from Mt. Fuji in Japan.